Transcriptomic analysis of vitamin D responses in uterine and peripheral NK cells

Tamblyn, Jennifer; Jeffery, Louisa; Susarla, Radhika; Lissauer, David; Coort, Susan L; Munoz Garcia, Amadeo; Knoblich, Konstantin; Fletcher, Anne; Bulmer, JN; Kilby, Mark; Hewison, Martin

DOI:
10.1530/REP-18-0509

Document Version
Peer reviewed version

Citation for published version (Harvard):
Tamblyn, J, Jeffery, L, Susarla, R, Lissauer, D, Coort, SL, Munoz Garcia, A, Knoblich, K, Fletcher, A, Bulmer, JN, Kilby, M & Hewison, M 2019, 'Transcriptomic analysis of vitamin D responses in uterine and peripheral NK cells', *Reproduction*, vol. 158, no. 2, pp. 211-221. https://doi.org/10.1530/REP-18-0509

 Accepted Manuscript published as REP-18-0509.R1. Accepted for publication: 03-Jun-2019

Transcriptomic analysis of vitamin D responses in uterine and peripheral NK cells

JA Tamblyn[1,2,3], LE Jeffery[1], R Susarla[1], DM Lissauer[1,2], SL Coort[4], A Muñoz Garcia[1,4], K Knoblich[,5], AL Fletcher[,5], JN Bulmer[6],, MD Kilby[1,2,3,7], M Hewison[1,3]

1. Institute of Metabolism and Systems Research, College of Medical and Dental Sciences, University of Birmingham, Birmingham, B15 2TT, UK
2. Centre for Women's & Newborn Health, Birmingham Health Partners, Birmingham Women's & Children's Foundation Hospital, Edgbaston, Birmingham, B15 2TG, UK
3. Centre for Endocrinology, Diabetes and Metabolism, Birmingham Health Partners, Birmingham, B15 2TT, UK
4. Department of Bioinformatics-BiGCaT, NUTRIM School for Nutrition and Translational Research in Metabolism, Maastricht University, Maastricht, 6229 ER, Netherlands
5. Biomedicine Discovery Institute, Monash University, Wellington Rd. Clayton VIC 3800 Australia
6. Reproductive and Vascular Biology Group, Institute of Cellular Medicine, Newcastle University, Newcastle upon Tyne, NE2 4HH
7. Fetal Medicine Centre, Birmingham Women's & Children's Foundation Trust, Edgbaston, Birmingham, B15 2TG, UK

Running title: Vitamin D and uterine natural killer cells

Key words: vitamin D, natural killer cells, decidua, peripheral blood, pregnancy

Word count: 3736

* Corresponding author:
Martin Hewison PhD
Institute of Metabolism & Systems Research
Level 2, IBR, Rm 225
The University of Birmingham

Birmingham, B15 2TT
UK
email: m.hewison@bham.ac.uk
Tel: +44 (0)121 414 6908 Fax: +44 (0) 121 415 8712

Abstract

Vitamin D deficiency is prevalent in pregnant women and is associated with adverse pregnancy outcomes, in particular disorders of malplacentation. The active form of vitamin D, 1,25-dihydroxyvitamin D3 ($1,25(OH)_2D3$), is a potent regulator of innate and adaptive immunity, but it's immune effects during pregnancy remain poorly understood. During early gestation, the predominant immune cells in maternal decidua are uterine natural killer cells (uNK), but the responsivity of these cells to $1,25(OH)_2D3$ is unknown despite high levels of $1,25(OH)_2D3$ in decidua. Transcriptomic responses to $1,25(OH)_2D3$ were characterised in paired donor uNK and peripheral natural killer cells (pNK) following cytokine (CK)-stimulation. RNAseq analyses indicated 911 genes were differentially expressed in CK-stimulated uNK versus CK-stimulated pNK in the absence of $1,25(OH)_2D3$, with predominant differentially-expressed pathways being associated with glycolysis and transforming growth factor β (TGFβ). RNAseq also showed that the vitamin D receptor (VDR) and its heterodimer partner retinoid X receptor were differentially-expressed in CK-stimulated uNK vs CK-stimulated pNK. Further analyses confirmed increased expression of VDR mRNA and protein, as well as VDR-RXR target in CK-stimulated uNK. RNAseq analysis showed that in CK-stimulated pNK, $1,25(OH)_2D3$ induced 38 and suppressed 33 transcripts, whilst in CK-stimulated uNK $1,25(OH)_2D3$ induced 46 and suppressed 19 genes. However, multiple comparison analysis of transcriptomic data indicated that 1,25(OH)2D3 had no significant overall effect on gene expression in either CK-stimulated pNK or uNK. These data indicate that CK-stimulated uNK are transcriptionally distinct from pNK and, despite expressing abundant VDR, neither pNK nor uNK are sensitive targets for vitamin D.

Word count: 249

 Accepted Manuscript published as REP-18-0509.R1. Accepted for publication: 03-Jun-2019

Introduction

Human implantation and placental development present a unique challenge for the maternal immune system (Taglauer, et al. 2010). From embryonic implantation, semi-allogeneic fetal extravillous trophoblast cells invade the maternal decidua and inner myometrium (including remodelling the spiral arteries) facilitating normal haemochorial placentation. Throughout these actions, the materno-fetal immune function remains active, with diverse mechanisms mounted to support fetal development and placentation (Abumaree, et al. 2012; Erlebacher 2013). From early pregnancy a high proportion of resident leukocytes, displaying unique phenotypes and functions reside within the uteroplacental interface (Bulmer, et al. 2010). CD56bright uterine natural killer cells (uNK) (60-70%) are predominant, appearing phenotypically distinct from CD56dim NK cells in peripheral blood (pNK) (<10% total circulating immune cell population). In addition to the classical pro-cytotoxic, anti-tumorigenic and anti-viral effects associated with pNK (Koopman, et al. 2003), uNK have also been shown to play a pivotal role in embryonic implantation and haemochorial placental development (Lash, et al. 2010).

Regulation of uNK function involves a complex network of factors (Szekeres-Bartho 2008), and we have postulated that vitamin D plays a role in this process. Vitamin D is a secosteroid that exerts powerful immuno-regulatory responses on cells from both the innate and adaptive immune systems following immune activation (Adams and Hewison 2008; Hewison 2011). Early in pregnancy, maternal concentrations of the active form of vitamin D, 1,25-dihydroxyvitamin D3 ($1,25(OH)_2D3$), increase dramatically (Tamblyn, et al. 2017). Moreover, the enzyme that catalyzes synthesis of $1,25(OH)_2D3$ from precursor 25-hydroxyvitamin D3 (25(OH)D3), 25-hydroxyvitamin D-1α-hydroxylase (CYP27B1) (Gray, et al. 1979; Weisman, et al. 1979; Zehnder, et al. 2002), as well as the nuclear vitamin D receptor (VDR) for $1,25(OH)_2D3$ (Zehnder et al. 2002), are abundantly expressed by both maternal decidua (stromal and immune cells) and fetal trophoblast (Evans, et al. 2004). The

precise targets for decidual 1,25$(OH)_2$D3 have yet to be defined, but may include effects upon VDR-expressing decidual immune cells (Zehnder et al. 2002). The aim of the current study was to characterise *ex vivo* the effects of 1,25$(OH)_2$D3 on gene expression in activated uNK from first trimester decidual tissue, and to contrast these changes with effects of 1,25$(OH)_2$D3 on paired pNK.

Materials and Methods

Ethical approval

Paired decidual and peripheral blood samples were obtained from healthy pregnant women undergoing 1st trimester elective surgical termination of pregnancy (TOP) (<12 weeks [w] gestational age [GA]; range 7-11^{+2} w) following written informed consent (2014–2017; NHS REC approval 06/Q2707/12 and 13/WM/0178). GA was determined by ultrasound measurement of crown rump length, and relevant anonymised patient demographics obtained as summarised (Supplemental Table 1).

Isolation of NK cells from peripheral blood and decidua

CD56+ cell-enriched isolates were prepared by modification of a previously published method (Lash, et al. 2006). Briefly, whole decidual tissue was minced and DNase/collagenase-treated. Lymphocyte purification was then carried out by density gradient centrifugation (Ficoll Plus, GE Healthcare Life Sciences, Little Chalfont, UK). For initial cell surface marker analysis, anti-CD56 reactive magnetic bead separation (MidiMACS, Miltenyi Biotec, Bisley, UK) was performed to obtain CD56+ cells.

Fluorescence Activated Cell Sorting (FACS)

For cell culture and RNAseq analysis, density-centrifuged cell populations were FACS sorted. Cells were surface stained with primary mAb as summarised and then washed in PBS and re-constituted in 500 µL MACS (PBS, pH 7.2, 0.5% bovine serum albumin (BSA), 2mM EDTA) for cell sorting. Propidium iodide (PI) was added to assess cell viability at the

 Accepted Manuscript published as REP-18-0509.R1. Accepted for publication: 03-Jun-2019

point of cell sorting, using a BD FACSAria Fusion Flow Cytometer (BD Biosciences, Wokingham, UK). The gating strategy for isolating live CD3-/CD56+ NK from peripheral blood and decidua is shown in Supplemental Figure 1. Live CD45+ CD3- CD14- CD56+ NKp46+ pNK and uNK were identified (overall purity ≥96%; pNK 99.0-99.2%, uNKs 96.0-98.7%). Monoclonal antibodies (mAb) used to gate live cells were: anti-CD56, anti-NKp46 (Miltenyi Biotec, Bisley, UK), anti-CD3, anti-CD8, anti-CD14 from BD Biosciences (San Jose, CA, USA). Isotype matched IgG and IgM controls conjugated to the appropriate fluorochrome (BD Bioscience, San Jose, CA, USA and eBioscience, Waltham, MA, USA) were used for non-specific binding.

Cell culture

Paired uNK and pNK were cultured in complete cell culture medium (Penstrep 100µg/ml, L-glutamine 2mM, RPMI 1640, fetal calf serum (10%) (Sigma-Aldrich, Irvine, UK) at 37°C and 5% CO_2 for 24 hours (h), as either unstimulated controls or with cytokine (CK) stimulation using recognised NK cell co-activators: IL-2 [50 IU/ mL], IL-12 [10 ng/ mL], and IL-15 [10 ng/ mL]). Unstimulated and CK uNK and pNK were cultured in the presence and absence of 1,25$(OH)_2$D3 (10nM)(Enzo Lifesciences, Exeter, UK) co-treatment.

Flow cytometric analysis of CD69 and VDR

Expression of VDR (D6 anti-VDR, Santa Cruz Biotechnology, Santa Cruz, CA, USA) and CD69 (anti-CD69, BD Biosciences, San Jose, CA, USA), a recognised surface marker of NK cell activation (Clausen, et al. 2003) was assessed in paired pNK and uNK following 24 h culture in the presence and absence of CK stimulation with or without 1,25$(OH)_2$D3. Briefly, cultured cells were harvested, washed in PBS and incubated with live/dead fixable discrimination dye (Thermo Fisher, Waltham, MA, USA) on ice for 30 min. Cells were washed with PBS, incubated for 30 min with surface primary mAb at 4°C and then re-washed. For intracellular VDR analysis, a protocol optimised from Bendix et al was used (Bendix, et al. 2015). Briefly, following surface staining cells were fixed for 20 min in 100 µL

4% PFA, washed twice in 2 mL 2% FCS-PBS, and incubated for 30 min on ice in 75 µL 5% FCS 0.5% Triton X solution (Sigma-Aldrich, Irvine, UK). Cells were then incubated with anti-VDR mAb for 30 min, washed with 2% FCS-PBS and re-incubated with anti-mouse IgG2a APC secondary mAb under the same conditions. Cells were then re-washed twice in 2% FCS-PBS followed by PBS and stored at 4°C prior to analysis. Flow cytometry data were collected using a multi-channel Dako Cyan flow cytometer (Beckman Coulter, High Wycombe, UK). Data were analysed using Flow Jo V10 (Tree star, Inc., Ashland, USA), gating live CD45+ CD56+ NKp46+ cells (Supplemental Figure 2). The specificity of the D6 anti-VDR mAb in VDR positive control cells (activated T cells) was demonstrated using flow cytometry, immunoprecipitation and chromatin immunoprecipitation (Supplemental Figure 3).

Confocal Imaging of VDR in CD56+ pNKs

CD56+ pNKs were isolated and stimulated overnight with CK in the presence of $1,25(OH)_2D3$ as described above. Cells were surface-labelled for CD56 using FITC-anti-CD56 (clone REA196 Miltenyi Biotec), then fixed and permeabilised for VDR labelling with mouse anti-human VDR (D6 clone, Santa Cruz Biotechnology, Santa Cruz, CA, USA) or mouse IgG2a isotype control according to the protocol described above for flow cytometry but with goat anti-mouse IgG2a-594 and goat-anti-FITC-488 (molecular probes, Fisher Scientific) secondary labelling for 30 mins in the presence of Hoechst 33342 (10 µg/ml; Fisher Scientific). After a final wash, cells were re-suspended in ProlongR Gold antifade reagent (Molecular Probes, Cell Signalling Technologies, UK) and placed under coverslip on charged microscope slides. Edges were sealed with nail varnish and 22-slice Z stack images of cells at 63x magnification, resolution 1024 x 1024 pixels per image were captured using the Zeiss LSM 880, Axio Observer confocal microscope and studied with Zen2012 software (Supplemental Figure 4).

 Accepted Manuscript published as REP-18-0509.R1. Accepted for publication: 03-Jun-2019

Quantitative real-time PCR (qRT-PCR) analysis

Total RNA was extracted as described previously (Jeffery, et al. 2012). cDNA was prepared by reverse transcription Taqman Reverse Transcription Reagents Kit (Applied Biosystems, Roche, Nersey, USA) as per manufacturer's instructions. qRT-PCR was performed on an ABI 7500 qPCR machine using Taqman assays from Applied Biosystems for VDR (Hs00172113_m1) and multiplexed with VIC labelled 18S rRNA (4319413E) (Applied Biosystems, Roche, Nersey, USA). Paired uNK and pNK gene expression following 24-hour culture in the presence and absence of CK-stimulation with and without $1,25(OH)_2D3$ co-treatment was measured. Relative expression compared to paired unstimulated pNK was assessed using fold-change calculated by the $2^{-\Delta\Delta Ct}$ method. All statistical analyses were carried out using Sigmaplot 9.0 software (Systat Inc., San Jose, CA, USA). Experimental means were compared statistically using one-way ANOVA, with the Holm-Sidak method used as a post hoc multiple-comparison procedure. Statistical analyses for RT-qPCR analyses were carried out using raw ΔCt values.

RNA sequence analysis (RNA-seq)

Total RNA was extracted using the RNeasy Micro Kit and RNeasy MinElute spin columns (QIAGEN, Hilden Germany), as per manufacturer's instructions, eluted in 15 µL RNAse-free water, and immediately stored at -80°C prior to library preparation and sequencing (Source Bioscience Facilities, Nottingham, UK). Following initial QC check using the Agilent BioAnalyzer 2100 (Agilent, Santa Clara, CA, USA) cDNA library preparation was performed using Switching Mechanism at the 5′ end of RNA Template (SMART)er Stranded Total RNA Seq Kit – Pico (Clontech, Mountain View, CA, USA) (RNA range = pg). Random primers and locked nucleic acid (LNA) technology were utilised to optimise total coverage. Illumina Adapters and Indexes (barcode markers) (Illumina, Inc., San Diego, USA) were added at PCR1 with rRNA cleaved by ZapR in the presence of R-Probes (mammalian-specific). The non-cleaved fragments underwent further enrichment in PCR2 cycle. All libraries were QC

validated using the Agilent BioAnalyzer 2100 (Santa Clara, CA, USA) to confirm index samples amplified concentration and size distribution. The libraries were pooled and re-validated to assess molarity and size distribution prior to loading (1.8pM concentration) onto a High Output NextSeq 500 Flow Cell pv2. (Illumina) across 4 lanes for RNA-seq using 75-base-pair (bp) paired-end reading, generating ~800 million total reads with an average of 25 million per sample. Raw data was returned in the FastQ Phred+33 (Illumina 1.9) format.

Bioinformatics and Pathway analysis

Bioinformatics analysis of RNA-seq analyses was performed at University of Birmingham, UK using Partek Flow Software (Partek, St Louis, Missouri, USA). Data were trimmed for adapter sequences and pre-alignment QA/QC was performed before being mapped (aligned) using STAR-2.4.1d (Dobin, et al. 2013). Post-alignment QA/QC was performed with a coverage report generated. Reads were quantified to transcriptome hg38_RefSeq (Genome Reference Consortium GRCh38), and normalised using quantile normalisation. Median total aligned reads was 71567649 (IQR; 64250828–74820738), representing 85.7% (84.5 – 87.5%) coverage**.** Differential gene expression was defined by a cut-off fold-change of < -1.5 and > 1.5, p-value ≤ 0.05 and false discovery rate (FDR)-step up ≤ 0.05. P-values were calculated using F-statistics, which calculates variance within samples. Three analyses were assessed: (i) CK uNK versus (vs) CK pNK; (ii) CK uNK vs CK uNK + 1,25$(OH)_2$D3; (iii) CK pNK vs CK pNK + 1,25$(OH)_2$D3.

Characterisation of common biological processes in the CK-activated uNK and pNK groups was carried out using PathVisio (Version 3.2.4), an open-source pathway analysis and visualization software tool for biological data analysis, using previously described protocols (Munoz Garcia, et al. 2018). Briefly, analysis was performed using the 11164 raw gene counts obtained, with corresponding ENTREZ ID and symbol from the HUGO Gene Nomenclature Committee (HGNC) identifiers. A p-value <0.05 was applied to determine differentially-expressed genes. The Z-Score, which signifies whether the total number of

 Accepted Manuscript published as REP-18-0509.R1. Accepted for publication: 03-Jun-2019

genes in the pathway are over-represented (Z-score >1.96) compared to the complete data set, was then calculated. The curated human pathway collection from the online-pathway repository WikiPathways (Kutmon, et al. 2016) including the Reactome (Bohler, et al. 2016) collection (downloaded May 2017) was used.

Results

Comparison of gene expression in cytokine (CK)-stimulated pNK and uNK cells

Principal Component Analysis (PCA) of unbiased genome-wide RNAseq analyses revealed wide variance in the transcriptional profiles of CK-stimulated uNK and pNK (Figure 1A). In both cell types, co-treatment with $1,25(OH)_2D3$ did not result in PCA separation of transcriptional profiles from their respective CK controls. Volcano plots of differentially expressed genes in CK-stimulated uNK relative to CK-stimulated pNK using a cut-off of $p \leq 0.05$ and fold change ≤-1.5 and ≥+1.5 showed 1098 up-regulated genes in CK-stimulated uNKs (red) and 1188 down-regulated genes (green), with those not significantly different in grey (n= 11163) (Figure 1B). Adjustment for false discovery rate (FDR) identified 911 transcripts to be differentially-expressed between CK-stimulated uNK and pNK, with 422 down-, and 489 up-regulated in CK-stimulated uNK relative to CK-stimulated pNK (*p* value ≤ 0.05; log2 fold-change ≤1.5 or ≥1.5, FDR step-up ≤ 0.05) (Figure 1C). Significantly regulated genes in CK-stimulated uNK relative to CK-stimulated pNK included up-regulation of *NCAM1* (CD56) (fold-change 5.29), and down-regulation of *FCG3RA* (CD16A) (fold change -14.57), both of which are well-recognised differentially expressed markers for CD56bright NK versus CD56dim pNK subsets (Koopman et al. 2003; Poli, et al. 2009b). Interestingly, granzyme (GZMK) (fold-change (7.83)) and CD96 (2.53), which permits adhesive interactions and modulates responses between activated T and NK cells (Georgiev, et al. 2018), were both up-regulated in CK-stimulated uNK. CD276 (7.71), a regulator of T cell cytotoxicity (Picarda, et al. 2016) was also up-regulated in CK uNK.

To better delineate the differences in transcript expression between CK-stimulated uNK and pNK, complementary pathway analysis was performed on FDR-adjusted differentially-expressed data using WikiPathways (WP) workflows. A broad spectrum of enriched canonical pathways was identified, with significantly enriched pathways ranked from a high to low Z-score (Supplemental Dataset 1). Pathways identified as being significantly enriched based on a Z-score ≥1.96 are shown in Table 1. Overall, 29 WP pathways were significantly enriched in CK-stimulated uNK relative to CK-stimulated pNK, including pathways related to hypoxia-inducible factor (HIF)1α and peroxisomal proliferator-activated receptor (PPAR)γ regulation of glycolysis, and transforming growth factor (TGF)α signalling (Supplemental Figures 5A-5S).

VDR expression in uNK is up-regulated following cytokine stimulation

RNA seq analysis revealed that VDR mRNA expression is significantly upregulated in CK stimulated uNK (fold change 8.56) relative to CK stimulated pNK. Analysis of differentially expressed pathways in CK-stimulated uNK versus CK-stimulated pNK in Supplemental Dataset 1 also showed enhanced expression of pathways associated with VDR and its heterodimer partner retinoid X receptor (RXR) (Z score 1.83, p=0.07) (Figure 2), as well as non-genomic actions of 1,25$(OH)_2$D3 (Z score 1.88, p=0.062) (Supplemental Figure 5A). This suggests that capacity for 1,25$(OH)_2$D3-VDR responses is elevated in CK-stimulated uNK relative to CK-stimulated pNK. Studies were therefore carried out to further characterise VDR expression in uNK and pNK. Flow cytometry showed that pNK and uNK expressed similar levels of the NK marker NKp46. Analysis of CD56 expression showed that uNK cells were characterised by more distinct populations of CD56bright and CD56dim cells than pNK (Figure 3A). Both CD56 and NKp46 showed no change in response to either CK stimulation or 1,25$(OH)_2$D3 treatment in either uNK or pNK cells for median fluorescence intensity (MFI) (Figure 3A) or frequency of expression (data not shown). As shown in Figure 3B and 3C, CK-stimulation significantly up-regulated expression of the activation marker CD69 in both uNK (median 47.9%; IQR 31.5-56.6 to 68.1%; 48.9-76.4) and pNK (17.7%; 11.5-20.3 to

 Accepted Manuscript published as REP-18-0509.R1. Accepted for publication: 03-Jun-2019

70.5%; 57.4-72.8), but treatment with 1,25$(OH)_2$D3 had no significant effect on CD69 expression in either the unstimulated or CK-stimulated uNK or pNK populations (Figure 3C).

Without stimulation the frequency of NK cells that expressed VDR was low for both uNK (36.2%; 33.1-36.5) and pNK (15.8%; 5.81-61.6). CK stimulation significantly increased VDR frequency in uNK (74.2%; 65.6-81.3) although the absolute level of VDR expression by each expressing cell (MFI) was not significantly increased (Figure 3D). 1,25$(OH)_2$D3 had no significant effect on VDR protein expression in either uNK or pNK in the presence or absence of CK-stimulation (Figure 3C). Expression of *VDR* mRNA was also significantly induced by CK-stimulation in uNK (p=0.0001) and pNK (p=0.017). Interestingly, this effect was suppressed in both cell types by co-treatment with 1,25$(OH)_2$D3 (Figure 3D). Confocal imaging of CK-stimulated pNK cells (Supplemental Figure 4) showed co-localization of VDR protein with both DNA (Hoescht staining) and the plasma membrane (CD56), consistent with both membrane and nuclear localisation of VDR.

Effects of 1,25$(OH)_2$D3 on gene expression in CK-stimulated pNK and uNK cells

When compared to CK-stimulated pNK, CK-stimulated pNK treated with 1,25$(OH)_2$D3, showed only 71 genes differentially-expressed genes (fold-change ±1.5; p≤0.05). Of these, 33 (46.5%) were down- and 38 (53.5%) up-regulated by 1,25$(OH)_2$D3. In CK-stimulated uNK treated with 1,25$(OH)_2$D3 66 genes were differentially-expressed relative to CK-stimulation of uNK alone. Of these, 46 (69.7%) were down- and 19 (30.3%) up-regulated by 1,25$(OH)_2$D3. In contrast to pNK, 1,25$(OH)_2$D3 primarily targeted uNK genes implicated in cell processing, specifically cell adhesion, apoptosis, migration and angiogenesis (n=27; 41.5%) (Table 2). Due to the relatively small number of genes differentially-expressed in response to 1,25$(OH)_2$D3 in either CK-stimulated pNK or uNK, adjustment of data to incorporate fold-change ±1.5, *p*-value ≤ 0.05, FDR-step up < 0.05 resulted in no significant effect of 1,25$(OH)_2$D3 for either CK-stimulated uNK or CK-stimulated pNK. Furthermore,

pathway analysis using non-adjusted differentially expressed gene data for either CK-stimulated uNK or CK-stimulated pNK cell treated with 1,25$(OH)_2$D3 showed no significant enrichment of any specific pathways by 1,25$(OH)_2$D3 (data not shown), and no commonality with any of the pathways that are known to be regulated by 1,25$(OH)_2$D3 in other immune cells (Figure 4).

Discussion

Previous studies using DNA microarrays have described transcriptomic variations in CD56bright pNK and CD56dim pNK cells, as well as CD56 bright uNK (Koopman et al. 2003). In the current study, pNK or uNK were not sub-categorized according to CD56 brightness, because CD56dim pNK predominate in peripheral blood (approximately 95% of total pNK cell population), whilst CD56bright uNK are the prevalent NK type in decidua (>95% of total uNK population). These differences imply that uNKs are constitutively active. In agreement with this, we observed that uNK were larger with abundant perforin and granzyme. Importantly, no change in CD56 or NKp46 activation receptor expression was measured in uNK or pNK in response to CK-stimulation or treatment with the active form of vitamin D, 1,25$(OH)_2$D3. CD56bright NKs are considered efficient immunomodulatory cytokine producers, and only become cytotoxic following appropriate activation. However, in contrast to NK from most other sites, uNKs do not express the activating receptor CD16 which mediates antibody-dependent cellular cytotoxicity (Poli, et al. 2009a). It appears that whilst uNKs maintain an intrinsic capacity to exert cytotoxic functions when specifically challenged, this function is regulated in normal early pregnancy (Moffett and Colucci 2014). Further undefined local mechanisms, such as cytokine or hormone secretion, or crosstalk with other immune cell types within the decidual micro-environment are also thought to suppress the potential lytic effects of uNKs (Hanna, et al. 2006). In the current study, pro-inflammatory IL-2, IL-12 and IL-15 were utilised for CK challenge, as these are recognised NK cell activators, with both IL-12 and IL-15 constitutively expressed within the decidua from initial implantation (Kovacs, et al. 1992; Zourbas, et al. 2001). Although IL-2 concentrations

 Accepted Manuscript published as REP-18-0509.R1. Accepted for publication: 03-Jun-2019

appear low within normal decidua (Jokhi, et al. 1994), significantly elevated IL-2 has been reported in the setting of malplacentation (Garzia, et al. 2013), where vitamin D-deficiency is also more common (Robinson, et al. 2011).

The first aim of the current study was to compare the transcriptomic profiles of uNK versus pNK following immune activation by CK-stimulation. The second objective of the study was to determine if CK-stimulated uNK and pNK were responsive to $1,25(OH)_2D3$ in a similar manner to that reported for other components of the immune system such as macrophages and T cells (Adams and Hewison 2008). Since the effects of $1,25(OH)_2D3$ on NK cell function in decidua and maternal blood are still unclear, NK cell subsets were not further sub-classified.

In the current study approximately 900 genes were differentially-expressed in CK-stimulated uNK versus CK-stimulated pNK, similar to previous DNA array analyses for unstimulated CD56dim pNK versus unstimulated CD56bright uNK (Koopman et al. 2003). In CK-stimulated uNK a comparable number of up- (429) and down-regulated (422) genes were measured when adjusted for FDR. By contrast, in the absence of CK-stimulation, it was reported that uNK almost exclusively exhibited enhanced transcription relative to pNK (Koopman et al. 2003). uNK responses to CK stimulation appear highly distinct from paired pNK. In the circulation, pNK function as an early cytolytic response to tumors or viral infection (Chiossone, et al. 2018; Vivier, et al. 2011). By contrast, consistent with previous reports, we observed that uNK are poorly cytolytic and express low levels of pNK cytokines such as interferon-γ (IFN-γ) and tumour necrosis factor-α (TNF-α) (Kopcow, et al. 2005; Vacca, et al. 2006), and appear less reactive with low CD107 (degranulation marker) expression relative to pNKs in response to CK challenge (data not published). The unique phenotype of uNK may reflect their adaptation within this unique maternal tissue microenvironment to aid decidualisation, embryonic implantation, and subsequent fetal development (Pollheimer, et al. 2018).

Detailed pathway analysis verified that CK-stimulated uNK are phenotypically distinct from CK-stimulated pNK, with cell metabolism, signalling and processing, and cancer pathways consistently over-expressed in CK-stimulated uNK relative to CK-stimulated pNK. These observations are consistent with the known roles of tissue-resident uNK in placental development and fetal implantation. The significant inter-pathway transcript variance between CK-stimulated uNK and pNK underlines the complex diversity of uNK cell function. HIF1A and PPARγ regulation of glycolysis (Z score 3.64) was the most significantly differentially-expressed pathway in CK-stimulated uNK (Supplemental Figure 5B). The Cori cycle, a lactate-glucose carbon recycling system between muscle and liver that decreases circulating lactate was also enriched in CK-stimulated uNK (Z score 3.33) Supplemental Figure 5D). Genes associated with glycolysis and gluconeogenesis were also enhanced in CK-activated uNK (Z score 1.83, 14/30 genes, p=0.067), further underlining the active metabolic remodelling in uNK relative to pNK. During early pregnancy decidualisation is associated with enhanced glucose influx (Frolova and Moley 2011; Kommagani, et al. 2013). Recent studies have shown that the decidua acts in a manner similar to that reported for tumors by generating energy via a high rate of glycolysis, even under aerobic conditions rather, than conventional oxidative phosphorylation (Zuo, et al. 2015). This is referred to as a decidual Warburg-like glycolysis similar to that reported in tumors and was dependent on expression of HIF1α and the lactate transporter protein (MCT4) (Zuo et al. 2015). Collectively, these data suggest that a key feature of activated uNK is to regulate glucose metabolism and lactate transport within the decidua. Dysregulation of glucose metabolism in the human uterus is associated with subfertility and aberrant implantation (Kommagani et al. 2013). Glycolytic flux targets in uNK may therefore represent novel translational strategies to precisely time and/or therapeutically extend the window of receptivity in women at high risk for early pregnancy loss. Consistent with previous microarray analysis of 1st trimester uNK and adult non-paired pNK (Wang, et al. 2014), the current study showed that CK-stimulated uNK are enriched for pathways associated with transcriptional regulation, which may serve

 Accepted Manuscript published as REP-18-0509.R1. Accepted for publication: 03-Jun-2019

to differentially regulate NK development and function in the decidual microenvironment. Whether pNK undergo significant transcriptional alterations following recruitment to the decidua or, alternatively, uNK represent an entirely distinct subset of NK cells remains unclear (Hanna, et al. 2003; Vacca, et al. 2011).

Of the total transcripts measured in CK activated uNK and pNK, only 66 (0.59%) and 71 (0.64%) respectively were significantly regulated by 1,25$(OH)_2$D3 ($p \leq 0.05$, fold change ± 1.5). Although transcriptomic analysis indicated that CK uNK and CK pNK respond differentially to 1,25$(OH)_2$D3, this effect was statistically insignificant as the current analysis was not significantly powered to account for multiple comparisons (FDR step up < 0.05). Sample size and participant heterogeneity are potential reasons for this. Intra-participant variability for pNK was high, whereas the uNK demonstrated comparatively low variability. The heterogeneity in pNK gene expression may be in part attributable to differences in gestational age, maternal age, ethnicity and smoking status (Supplemental Table I), albeit n numbers are small. Cellular heterogeneity may also be a contributing factor to sample variability as recent single cell RNA sequencing data indicates 3 highly distinct decidual NK subsets to be resident within first trimester decidua (Vento-Tormo, et al. 2018).

Analysis of commonly regulated biological pathways, as detailed previously (Munoz Garcia et al. 2018), demonstrates that responses to 1,25$(OH)_2$D3 in CK-stimulated uNK and pNK diverge significantly from other immune subsets including monocytes, dendritic cells and B cells (Figure 4). This may in part reflect different treatment regimens. Here a physiological treatment dose (10nM) of 1,25$(OH)_2$D3 was utilised, whereas for monocytic THP-1 cells a 10-fold higher treatment dose (100nM) was applied (Seuter, et al. 2016). Temporal variations may also be a contributory factor. For THP-1 cells 46 genes were induced/ suppressed after 2.5 h, 288 at 4 h and 1204 at 24 h. In the current study we assessed mRNA expression in NK cells after 24 h to maximise potential variations in gene expression, however both pNK and uNK cells may show different patterns of gene regulation by

$1,25(OH)_2D3$ at earlier or later time points. The distinct transcriptional responses to $1,25(OH)_2D3$ by NK cells may also reflect differential distribution of VDR.

Data reported here provide further evidence for the distinct phenotype of uNK cells relative to circulating pNK. By comparing the gene expression profile of these cells under conditions of immune activation, we confirmed enrichment of distinct functional pathways in uNK such as TGF-β signalling (Supplemental Figure 5C) which has previously been shown to promote uNK development (Keskin, et al. 2007). Our data have also revealed novel features of CK-stimulated uNK, notably enrichment of pathways associated with metabolism, suggesting a role for uNK cells in immunometabolic activity within the decidua. The lack of $1,25(OH)_2D3$ response by uNK and pNK contrasts the expression of VDR by both cell types and the enhancement of this receptor in CK-stimulated uNK vs pNK. Given the abundant levels of $1,25(OH)_2D3$ within decidual tissue (Tamblyn et al. 2017), and the potent immunomodulatory actions of $1,25(OH)_2D3$ (Chun, et al. 2014), the lack of response by NK cells is intriguing. Further studies are required to better define the role of the VDR in NK cells. Data in the current study suggest possible cell membrane expression of VDR and this may support non-genomic responses to $1,25(OH)_2D3$ (Hii and Ferrante 2016). In the case of uNK, it is also possible that $1,25(OH)_2D3$ is able to influence these cells indirectly via other immune cells such as macrophages that have an established transcriptional and functional response to $1,25(OH)_2D3$. It is now clear that uNK play a key role in mediating the cross-talk between immune cells within the decidua (Vento-Tormo et al. 2018), and vitamin D may therefore play a role in this process. Finally, the data presented in the current study have focused on transcriptional activity but it is also possible that $1,25(OH)_2D3$ exerts epigenetic effects on NK cells independent of transcription. In recent studies of uNK cells it has been shown that repeated pregnancies are associated with uNK cells that have a unique transcriptomic and epigenetic signature consistent with trained immune responses (Gamliel, et al. 2018). Based on its established epigenetic activity (Carlberg 2019), it is tempting to speculate that vitamin D may contribute to this facet of uNK function.

 Accepted Manuscript published as REP-18-0509.R1. Accepted for publication: 03-Jun-2019

Declaration of Interest

The authors declare that there is no conflict of interest that could be perceived as prejudicing the impartiality of the research reported. Vitabiotics Pregnacare generously supported this work through the charity Wellbeing of Women, which independently selected the research through its AMRC accredited peer review process led by its Research Advisory Committee. Dr Tamblyn and her work were not impacted or influenced in any way by its sources of funding.

Study funding

This study was supported by funding from NIH (AR063910, MH), a Royal Society Wolfson Merit Award (MH), Mason Medical Trust (JAT), and Wellbeing of Women (RTF401, JAT).

Acknowledgments

We would like to thank Matt MacKenzie for help with flow cytometry cell sorting, and Scott P. Davies and Jennifer L. Marshall for help with confocal imaging.

References

Abumaree MH, Chamley LW, Badri M & El-Muzaini MF 2012 Trophoblast debris modulates the expression of immune proteins in macrophages: a key to maternal tolerance of the fetal allograft? *J Reprod Immunol* **94** 131-141.

Adams JS & Hewison M 2008 Unexpected actions of vitamin D: new perspectives on the regulation of innate and adaptive immunity. *Nat Clin Pract Endocrinol Metab* **4** 80-90.

Bendix M, Dige A, Deleuran B, Dahlerup JF, Peter Jorgensen S, Bartels LE, Husted LB, Harslof T, Langdahl B & Agnholt J 2015 Flow cytometry detection of vitamin D receptor changes during vitamin D treatment in Crohn's disease. *Clin Exp Immunol*. **181** 19-28

Bohler A, Wu G, Kutmon M, Pradhana LA, Coort SL, Hanspers K, Haw R, Pico AR & Evelo CT 2016 Reactome from a WikiPathways Perspective. *PLoS Comput Biol* **12** e1004941.

Bulmer JN, Williams PJ & Lash GE 2010 Immune cells in the placental bed. *Int J Dev Biol* **54** 281-294.

Carlberg C 2019 Nutrigenomics of Vitamin D. *Nutrients* **11** E676.

Chiossone L, Dumas PY, Vienne M & Vivier E 2018 Natural killer cells and other innate lymphoid cells in cancer. *Nat Rev Immunol* **18** 671-688.

Chun RF, Liu PT, Modlin RL, Adams JS & Hewison M 2014 Impact of vitamin D on immune function: Lessons learned from genome-wide analysis **5** 151.

Clausen J, Vergeiner B, Enk M, Petzer AL, Gastl G & Gunsilius E 2003 Functional significance of the activation-associated receptors CD25 and CD69 on human NK-cells and NK-like T-cells. *Immunobiology* **207** 85-93.

Dobin A, Davis CA, Schlesinger F, Drenkow J, Zaleski C, Jha S, Batut P, Chaisson M & Gingeras TR 2013 STAR: ultrafast universal RNA-seq aligner. *Bioinformatics* **29** 15-21.

Erlebacher A 2013 Immunology of the maternal-fetal interface. *Annu Rev Immunol* **31** 387-411.

Evans KN, Bulmer JN, Kilby MD & Hewison M 2004 Vitamin D and placental-decidual function. *J Soc Gynecol Investig* **11** 263-271.

Frolova AI & Moley KH 2011 Quantitative analysis of glucose transporter mRNAs in endometrial stromal cells reveals critical role of GLUT1 in uterine receptivity. *Endocrinology* **152** 2123-2128.

Gamliel M, Goldman-Wohl D, Isaacson B, Gur C, Stein N, Yamin R, Berger M, Grunewald M, Keshet E, Rais Y, et al. 2018 Trained Memory of Human Uterine NK

 Accepted Manuscript published as REP-18-0509.R1. Accepted for publication: 03-Jun-2019

Cells Enhances Their Function in Subsequent Pregnancies. *Immunity* **48** 951-962 e955.

Garzia E, Clauser R, Persani L, Borgato S, Bulfamante G, Avagliano L, Quadrelli F & Marconi AM 2013 Prolactin and proinflammatory cytokine expression at the fetomaternal interface in first trimester miscarriage. *Fertil Steril* **100** 108-115 e101-102.

Georgiev H, Ravens I, Papadogianni G & Bernhardt G 2018 Coming of Age: CD96 Emerges as Modulator of Immune Responses. *Front Immunol* **9** 1072.

Gray TK, Lester GE & Lorenc RS 1979 Evidence for extra-renal 1 alpha-hydroxylation of 25-hydroxyvitamin D3 in pregnancy. *Science* **204** 1311-1313.

Hanna J, Goldman-Wohl D, Hamani Y, Avraham I, Greenfield C, Natanson-Yaron S, Prus D, Cohen-Daniel L, Arnon TI, Manaster I, et al. 2006 Decidual NK cells regulate key developmental processes at the human fetal-maternal interface. *Nat Med* **12** 1065-1074.

Hanna J, Wald O, Goldman-Wohl D, Prus D, Markel G, Gazit R, Katz G, Haimov-Kochman R, Fujii N, Yagel S, et al. 2003 CXCL12 expression by invasive trophoblasts induces the specific migration of CD16- human natural killer cells. *Blood* **102** 1569-1577.

Hewison M 2011 Antibacterial effects of vitamin D. *Nat Rev Endocrinol* **7** 337-345.

Hii CS & Ferrante A 2016 The Non-Genomic Actions of Vitamin D. *Nutrients* **8** 135.

Jeffery LE, Wood AM, Qureshi OS, Hou TZ, Gardner D, Briggs Z, Kaur S, Raza K & Sansom DM 2012 Availability of 25-Hydroxyvitamin D3 to APCs Controls the Balance between Regulatory and Inflammatory T Cell Responses. *J Immunol* **189** 5155-5164.

Jokhi PP, King A, Sharkey AM, Smith SK & Loke YW 1994 Screening for cytokine messenger ribonucleic acids in purified human decidual lymphocyte populations by the reverse-transcriptase polymerase chain reaction. *J Immunol* **153** 4427-4435.

Keskin DB, Allan DS, Rybalov B, Andzelm MM, Stern JN, Kopcow HD, Koopman LA & Strominger JL 2007 TGFbeta promotes conversion of CD16+ peripheral blood NK cells into CD16- NK cells with similarities to decidual NK cells. *Proc Natl Acad Sci U S A* **104** 3378-3383.

Kommagani R, Szwarc MM, Kovanci E, Gibbons WE, Putluri N, Maity S, Creighton CJ, Sreekumar A, DeMayo FJ, Lydon JP, et al. 2013 Acceleration of the glycolytic flux by steroid receptor coactivator-2 is essential for endometrial decidualization. *PLoS Genet* **9** e1003900.

Koopman LA, Kopcow HD, Rybalov B, Boyson JE, Orange JS, Schatz F, Masch R, Lockwood CJ, Schachter AD & Park PJ 2003 Human decidual natural killer cells are

a unique NK cell subset with immunomodulatory potential. *The Journal of experimental medicine* **198** 1201-1212.

Kopcow HD, Allan DS, Chen X, Rybalov B, Andzelm MM, Ge B & Strominger JL 2005 Human decidual NK cells form immature activating synapses and are not cytotoxic. *Proc Natl Acad Sci U S A* **102** 15563-15568.

Kovacs E, Meichsner-Frauli M & Ludwig H 1992 Interleukin-2 receptor positive cells in human decidua during the first trimester of pregnancy and their association with macrophages. *Arch Gynecol Obstet* **251** 93-100.

Kutmon M, Riutta A, Nunes N, Hanspers K, Willighagen EL, Bohler A, Melius J, Waagmeester A, Sinha SR, Miller R, et al. 2016 WikiPathways: capturing the full diversity of pathway knowledge. *Nucleic Acids Res* **44** D488-494.

Lash GE, Otun HA, Innes BA, Percival K, Searle RF, Robson SC & Bulmer JN 2010 Regulation of extravillous trophoblast invasion by uterine natural killer cells is dependent on gestational age. *Hum Reprod* **25** 1137-1145.

Lash GE, Schiessl B, Kirkley M, Innes BA, Cooper A, Searle RF, Robson SC & Bulmer JN 2006 Expression of angiogenic growth factors by uterine natural killer cells during early pregnancy. *J Leukoc Biol* **80** 572-580.

Moffett A & Colucci F 2014 Uterine NK cells: active regulators at the maternal-fetal interface. *J Clin Invest* **124** 1872-1879.

Munoz Garcia A, Kutmon M, Eijssen L, Hewison M, Evelo CT & Coort SL 2018 Pathway analysis of transcriptomic data shows immunometabolic effects of vitamin D. *J Mol Endocrinol* **60** 95-108.

Picarda E, Ohaegbulam KC & Zang X 2016 Molecular Pathways: Targeting B7-H3 (CD276) for Human Cancer Immunotherapy. *Clin Cancer Res* **22** 3425-3431.

Poli A, Michel T, Theresine M, Andres E, Hentges F & Zimmer J 2009a CD56bright natural killer (NK) cells: an important NK cell subset. *Immunology* **126** 458-465.

Poli A, Michel T, Thérésine M, Andrès E, Hentges F & Zimmer J 2009b CD56(bright) natural killer (NK) cells: an important NK cell subset. *Immunology* **126** 458-465.

Pollheimer J, Vondra S, Baltayeva J, Beristain AG & Knofler M 2018 Regulation of Placental Extravillous Trophoblasts by the Maternal Uterine Environment. *Front Immunol* **9** 2597.

Robinson CJ, Wagner CL, Hollis BW, Baatz JE & Johnson DD 2011 Maternal vitamin D and fetal growth in early-onset severe preeclampsia. *Am J Obstet Gynecol* **204** 556 e551-554.

Seuter S, Neme A & Carlberg C 2016 Epigenome-wide effects of vitamin D and their impact on the transcriptome of human monocytes involve CTCF. *Nucleic Acids Res* **44** 4090-4104.

 Accepted Manuscript published as REP-18-0509.R1. Accepted for publication: 03-Jun-2019

Szekeres-Bartho J 2008 Regulation of NK cell cytotoxicity during pregnancy. *Reprod Biomed Online* **16** 211-217.

Taglauer ES, Adams Waldorf KM & Petroff MG 2010 The hidden maternal-fetal interface: events involving the lymphoid organs in maternal-fetal tolerance. *The International journal of developmental biology* **54** 421-430.

Tamblyn JA, Susarla R, Jenkinson C, Jeffery LE, Ohizua O, Chun RF, Chan SY, Kilby MD & Hewison M 2017 Dysregulation of maternal and placental vitamin D metabolism in preeclampsia. *Placenta* **50** 70-77.

Vacca P, Moretta L, Moretta A & Mingari MC 2011 Origin, phenotype and function of human natural killer cells in pregnancy. *Trends Immunol* **32** 517-523.

Vacca P, Pietra G, Falco M, Romeo E, Bottino C, Bellora F, Prefumo F, Fulcheri E, Venturini PL, Costa M, et al. 2006 Analysis of natural killer cells isolated from human decidua: Evidence that 2B4 (CD244) functions as an inhibitory receptor and blocks NK-cell function. *Blood* **108** 4078-4085.

Vento-Tormo R, Efremova M, Botting RA, Turco MY, Vento-Tormo M, Meyer KB, Park JE, Stephenson E, Polanski K, Goncalves A, et al. 2018 Single-cell reconstruction of the early maternal-fetal interface in humans. *Nature* **563** 347-353.

Vivier E, Raulet DH, Moretta A, Caligiuri MA, Zitvogel L, Lanier LL, Yokoyama WM & Ugolini S 2011 Innate or adaptive immunity? The example of natural killer cells. *Science* **331** 44-49.

Wang F, Zhou Y, Fu B, Wu Y, Zhang R, Sun R, Tian Z & Wei H 2014 Molecular signatures and transcriptional regulatory networks of human immature decidual NK and mature peripheral NK cells. *Eur J Immunol* **44** 2771-2784.

Weisman Y, Harell A, Edelstein S, David M, Spirer Z & Golander A 1979 1 alpha, 25-Dihydroxyvitamin D3 and 24,25-dihydroxyvitamin D3 in vitro synthesis by human decidua and placenta. *Nature* **281** 317-319.

Zehnder D, Evans KN, Kilby MD, Bulmer JN, Innes BA, Stewart PM & Hewison M 2002 The ontogeny of 25-hydroxyvitamin D(3) 1alpha-hydroxylase expression in human placenta and decidua. *Am J Pathol* **161** 105-114.

Zourbas S, Dubanchet S, Martal J & Chaouat G 2001 Localization of pro-inflammatory (IL-12, IL-15) and anti-inflammatory (IL-11, IL-13) cytokines at the foetomaternal interface during murine pregnancy. *Clin Exp Immunol* **126** 519-528.

Zuo RJ, Gu XW, Qi QR, Wang TS, Zhao XY, Liu JL & Yang ZM 2015 Warburg-like Glycolysis and Lactate Shuttle in Mouse Decidua during Early Pregnancy. *J Biol Chem* **290** 21280-21291.

Figure Legends

Figure 1. Transcriptomic analysis of cytokine (CK) stimulated pNK and uNK cells.

A. Principal component analysis (PCA) analysis of CK-stimulated uNK and pNKs in the presence and absence of $1,25(OH)_2D3$. 3-dimensional dot-plot summarising the main sources of variance across the whole RNA-seq data set by principal components; PC1 29.9%, PC2 11.9%, PC3 9.3%. This includes pNK (red), uNK (blue) in the presence (small dot) and absence (large dot) of $1,25(OH)_2D3$ co-treatment. B. Volcano plot summary of differentially expressed genes in CK-stimulated uNK relative to CK-stimulated pNK. Significantly up-regulated genes in CK-stimulated uNKs are in red (n=1098), down-regulated genes in green (n=1188), with those not significantly different in grey (n= 11163). A cut-off of $p \leq 0.05$ and fold change ≤-1.5 or ≥+1.5 was used to determine significance. C. Venn diagram summarising the distribution of differentially-expressed genes in CK-stimulated uNK relative to CK-stimulated pNK compared to total transcripts in CK-stimulated uNK and CK pNK following adjustment for false discover rate (FDR): p value ≤ 0.05; log2 fold-change ≤1.5 or ≥1.5, FDR step-up ≤ 0.05.

Figure 2. Pathway analysis of vitamin D receptor (VDR) signalling-related genes in CK-stimulated uNK versus CK-stimulated pNK. Visualisation of genes with enhanced (red) or suppressed (blue) expression in CK-stimulated uNK versus CK-stimulated pNK. Individual genes are shown in boxes and box colour split into two parts, (1) the log2 fold-change in the left part of the box (blue down-regulated, white not changed, red up-regulated) and (2) *p*-value for statistical significance is shown in the right part of the box (green when significant). Pathway elements not assessed in the dataset are shown in grey.

Figure 3. Expression of VDR in paired peripheral blood and uterine natural killer cells

A. Representative flow cytometry plots for expression of NKp46 and CD56 in isolated unstimulated (US) and cytokine (CK)-stimulated peripheral blood natural killer cells (pNK) and uterine natural killer cells (uNK) relative to isotype control (Iso). B. Representative flow

 Accepted Manuscript published as REP-18-0509.R1. Accepted for publication: 03-Jun-2019

cytometry plots for expression of VDR and CD69 in US and CK-stimulated CD3-CD56+ uNK and pNK cells relative to Iso control. C. Summary of VDR and CD69 surface protein expression in US- and CK-uNK and -pNK cells in the presence or absence of $1,25(OH)_2D3$ (1,25D). D. Median fluorescence intensity (MFI) for VDR expression in pNK and uNK cells. E. mRNA expression for *VDR* in isolated US and CK uNK and pNK cells in the presence and absence of $1,25(OH)_2D3$. Relative expression compared to US uNK cells; median value with bars denoting inter-quartile range. Effect of CK stimulation and $1,25(OH)_2D3$ was assessed by two-way ANOVA. . Stars indicate level of significant difference between groups for which multiple comparisons analysis indicated significance *<0.05, **<0.01.

Figure 4. **Pathway analysis of transcriptomic responses to $1,25(OH)_2D3$-treated in THP-1 cells, dendritic cells, monocytes and B cells compared to effects in pNK and uNK**. Heat map representing Z-scores for pathways significantly altered by $1,25(OH)_2D3$ comparing pathway analysis on datasets from THP-1 cells, dendritic cells (DC), monocytes and B cells with effects of $1,25(OH)_2D3$ on CK-stimulated pNK and uNK. Z-scores >1.96 indicate that more genes are significantly altered in this pathway compared to the complete dataset. Genes differentially expressed between CK-stimulated uNK and pNK in the absence of $1,25(OH)_2D3$ (pNK vs uNK) showed minimal overlap with the effect of $1,25(OH)_2D3$ on immune cells. The effects of $1,25(OH)_2D3$ on CK-stimulated pNK or uNK showed no commonality with the other immune cells.

Table 1. Pathway analysis of differential gene expression in CK uNK versus CK pNK

Summary of WikiPathways data-base analysis for CK-stimulated uNK versus CK-stimulated pNK. Frequency of significant differentially-expressed genes, total genes measured as a proportion of the total frequency of pathway enriched genes (*p*-value <0.05, Z-Score >1.96).

Table 2. Effect of $1,25(OH)_2D3$ on gene expression in CK pNK and uNK. Summary of total genes differentially induced or suppressed by $1,25(OH)_2D3$ in CK-stimulated pNK and

CK-stimulated uNK (fold change < -1.5 or > +1.5, $p \leq 0.05$), with sub-categorisation according to transcript function.

Accepted Manuscript published as REP-18-0509.R1. Accepted for publication: 03-Jun-2019

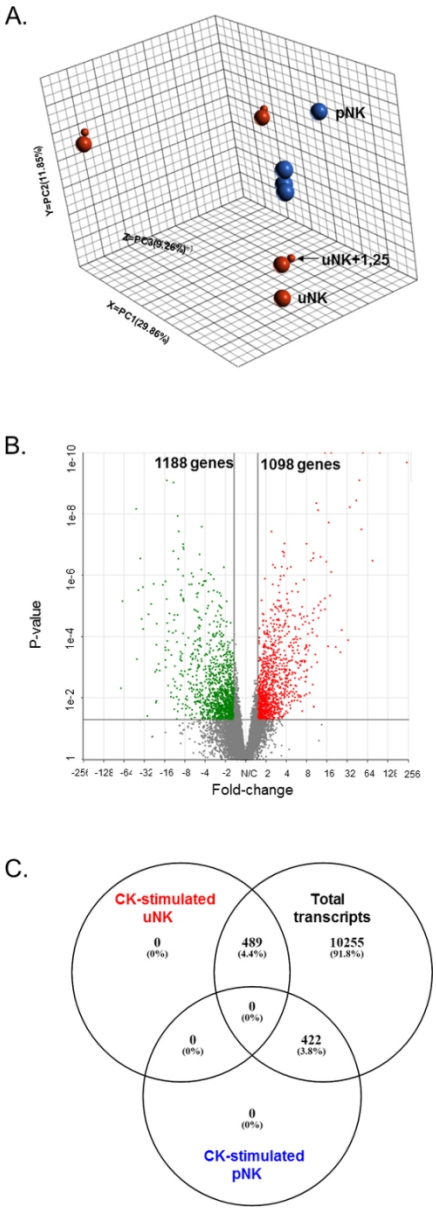

Figure 1. Transcriptomic analysis of cytokine (CK) stimulated pNK and uNK cells.
A. Principal component analysis (PCA) analysis of CK-stimulated uNK and pNKs in the presence and absence of 1,25(OH)2D3. 3-dimensional dot-plot summarising the main sources of variance across the whole RNA-seq data set by principal components; PC1 29.9%, PC2 11.9%, PC3 9.3%. This includes pNK (red), uNK (blue) in the presence (small dot) and absence (large dot) of 1,25(OH)2D3 co-treatment. B. Volcano plot summary of differentially expressed genes in CK-stimulated uNK relative to CK-stimulated pNK. Significantly up-regulated genes in CK-stimulated uNKs are in red (n=1098), down-regulated genes in green (n=1188), with those not significantly different in grey (n= 11163). A cut-off of p≤0.05 and fold change ≤-1.5 or ≥+1.5 was used to determine significance. C. Venn diagram summarising the distribution of differentially-expressed genes in CK-stimulated uNK relative to CK-stimulated pNK compared to total transcripts in CK-stimulated uNK and CK pNK following adjustment for false discover rate (FDR): p value ≤ 0.05; log2 fold-change ≤1.5 or ≥1.5, FDR step-up ≤ 0.05.

46x129mm (300 x 300 DPI)

Accepted Manuscript published as REP-18-0509.R1. Accepted for publication: 03-Jun-2019

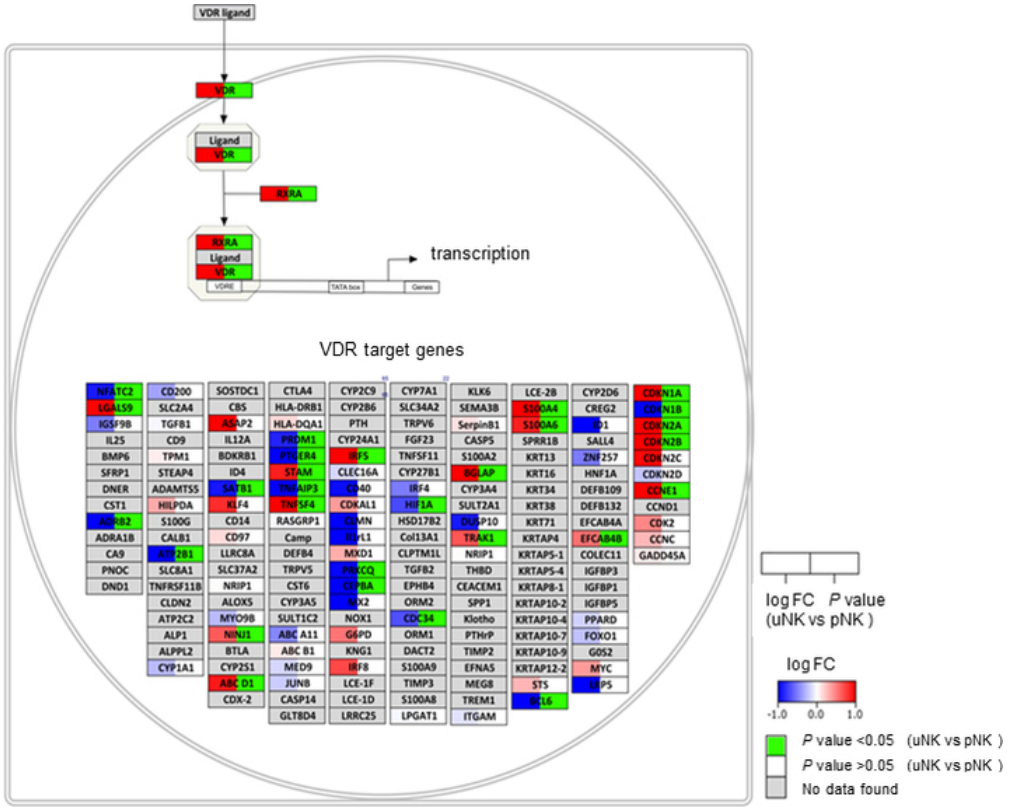

Figure 2. Pathway analysis of vitamin D receptor (VDR) signalling-related genes in CK-stimulated uNK versus CK-stimulated pNK. Visualisation of genes with enhanced (red) or suppressed (blue) expression in CK-stimulated uNK versus CK-stimulated pNK. Individual genes are shown in boxes and box colour split into two parts, (1) the log2 fold-change in the left part of the box (blue down-regulated, white not changed, red up-regulated) and (2) p-value for statistical significance is shown in the right part of the box (green when significant). Pathway elements not assessed in the dataset are shown in grey.

60x48mm (300 x 300 DPI)

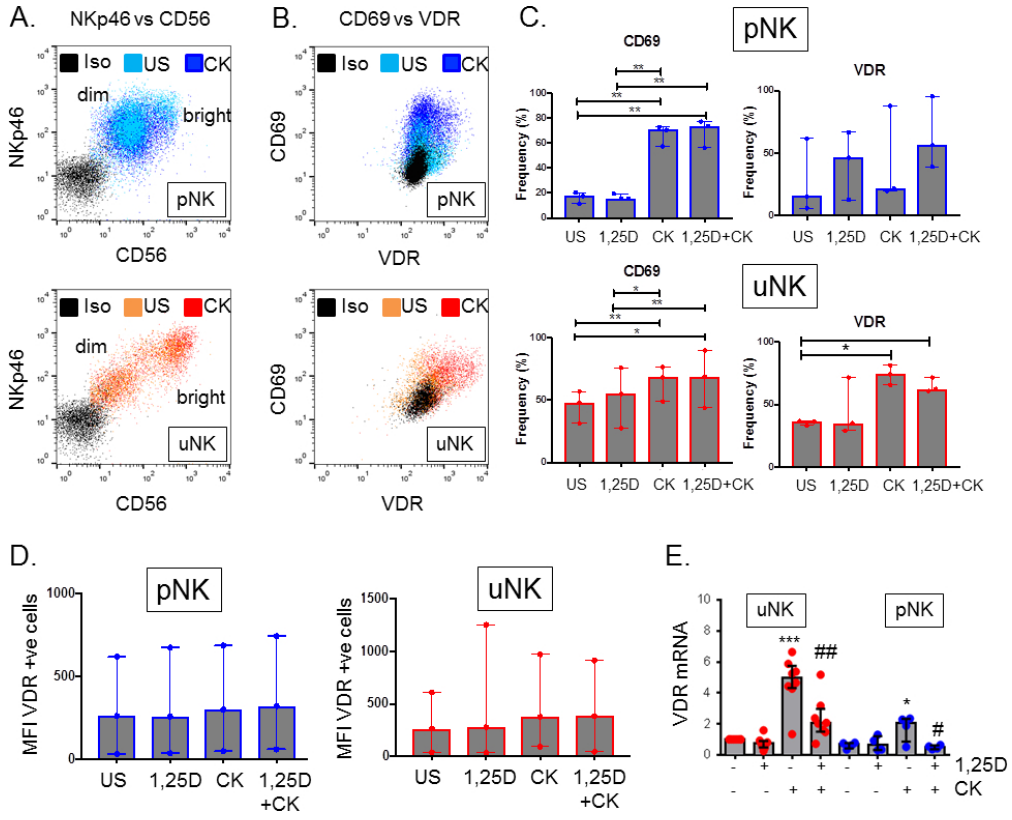

Figure 3. Expression of VDR in paired peripheral blood and uterine natural killer cells A. Representative flow cytometry plots for expression of NKp46 and CD56 in isolated unstimulated (US) and cytokine (CK)-stimulated peripheral blood natural killer cells (pNK) and uterine natural killer cells (uNK) relative to isotype control (Iso). B. Representative flow cytometry plots for expression of VDR and CD69 in US and CK-stimulated CD3-CD56+ uNK and pNK cells relative to Iso control. C. Summary of VDR and CD69 surface protein expression in US- and CK-uNK and -pNK cells in the presence or absence of 1,25(OH)2D3 (1,25D). D. Median fluorescence intensity (MFI) for VDR expression in pNK and uNK cells. E. mRNA expression for VDR in isolated US and CK uNK and pNK cells in the presence and absence of 1,25(OH)2D3. Relative expression compared to US uNK cells; median value with bars denoting inter-quartile range. Effect of CK stimulation and 1,25(OH)2D3 was assessed by two-way ANOVA. . Stars indicate level of significant difference between groups for which multiple comparisons analysis indicated significance *<0.05, **<0.01.

81x65mm (300 x 300 DPI)

Accepted Manuscript published as REP-18-0509.R1. Accepted for publication: 03-Jun-2019

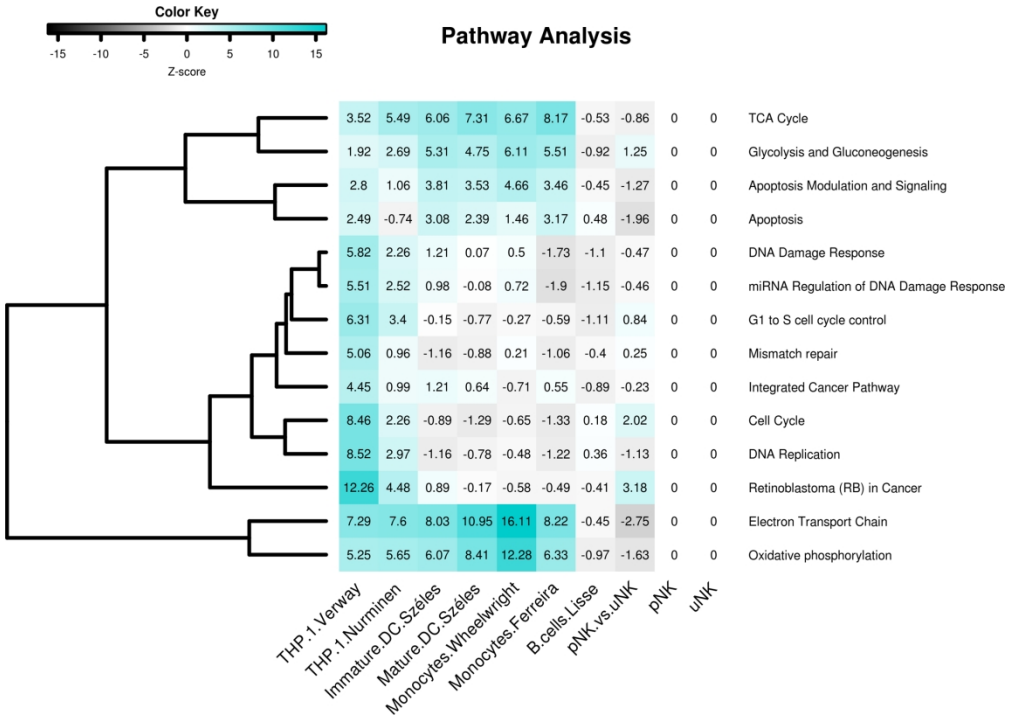

Figure 4. Pathway analysis of transcriptomic responses to 1,25(OH)2D3-treated in THP-1 cells, dendritic cells, monocytes and B cells compared to effects in pNK and uNK. Heat map representing Z-scores for pathways significantly altered by 1,25(OH)2D3 comparing pathway analysis on datasets from THP-1 cells, dendritic cells (DC), monocytes and B cells with effects of 1,25(OH)2D3 on CK-stimulated pNK and uNK. Z-scores >1.96 indicate that more genes are significantly altered in this pathway compared to the complete dataset. Genes differentially expressed between CK-stimulated uNK and pNK in the absence of 1,25(OH)2D3 (pNK vs uNK) showed minimal overlap with the effect of 1,25(OH)2D3 on immune cells. The effects of 1,25(OH)2D3 on CK-stimulated pNK or uNK showed no commonality with the other immune cells.

213x151mm (300 x 300 DPI)

Pathway	positive	measured	total	% positive	Z Score	p-value
HIF1A and PPARG regulation of glycolysis	6	6	19	100.00%	3.64	0
TGF-beta Signaling Pathway	51	111	133	45.95%	3.38	0.003
Cori Cycle	8	10	53	80.00%	3.33	0
Gastric Cancer Network 1	14	22	30	63.64%	3.29	0.001
Retinoblastoma Gene in Cancer	38	80	98	47.50%	3.16	0.001
Extracellular vesicle-mediated signaling in recipient cells	12	19	31	63.16%	3.01	0
Regulation of sister chromatid separation at metaphase-anaphase transition	10	15	16	66.67%	2.96	0.004
Calcium Regulation in the Cardiac Cell	31	65	164	47.69%	2.88	0.003
Primary Focal Segmental Glomerulosclerosis FSGS	20	38	78	52.63%	2.86	0.003
Fluoropyrimidine Activity	13	22	58	59.09%	2.82	0.001
Integrin-mediated Cell Adhesion	30	64	102	46.88%	2.72	0.004
Focal Adhesion	46	108	201	42.59%	2.57	0.014
Chemokine signaling pathway	42	99	172	42.42%	2.42	0.024
Ebola Virus Pathway on Host	39	91	141	42.86%	2.41	0.018
B Cell Receptor Signaling Pathway	36	83	99	43.37%	2.4	0.009
Nanoparticle-mediated activation of receptor signaling	12	22	36	54.55%	2.36	0.016
Lamin A-processing pathway	4	5	8	80.00%	2.35	0.015
Signal Transduction of S1P Receptor	11	20	26	55.00%	2.3	0.022
MFAP5-mediated ovarian cancer cell motility and invasiveness	6	9	18	66.67%	2.29	0.026
Microglia Pathogen Phagocytosis Pathway	15	30	44	50.00%	2.22	0.027
Histone Modifications	27	61	68	44.26%	2.21	0.024
Association Between Physico-Chemical Features & Toxicity Associated Pathways	22	48	78	45.83%	2.19	0.026
Human Thyroid Stimulating Hormone (TSH) signaling pathway	24	54	67	44.44%	2.1	0.032
Mesodermal Commitment Pathway	35	84	154	41.67%	2.08	0.024
Apoptosis-related network due to altered Notch3 in ovarian cancer	20	44	54	45.45%	2.04	0.047
Regulation of Wnt/B-catenin Signaling by Small Molecule Compounds	7	12	33	58.33%	2.03	0.036
T-Cell antigen Receptor (TCR) Signaling Pathway	32	77	93	41.56%	1.97	0.047
Purine metabolism	6	10	75	60.00%	1.96	0.044
G Protein Signaling Pathways	25	58	97	43.10%	1.96	0.047

Table 1. Pathway analysis of differential gene expression in CK uNK versus CK pNK

Summary of WikiPathways data-base analysis for CK uNK versus CK pNK. Frequency of significant differentially-expressed genes (*p*-value <0.05, Z-Score >1.96), total genes measured as a proportion of the total frequency of pathway enriched genes were ranked based on Z score.

Accepted Manuscript published as REP-18-0509.R1. Accepted for publication: 03-Jun-2019

Table 2

Functional classification	Genes expressed in pNK			Genes expressed in uNK		
	Total transcripts	Up-regulated by $1,25(OH)_2D3$	Down-regulated by $1,25(OH)_2D3$	Total transcripts	Up-regulated by $1,25(OH)_2D3$	Down-regulated by $1,25(OH)_2D3$
Cell structure	3	*TTLL1, FAM161A*	CMYA5	2		CAMSAP2, SOBP
Cell survival, proliferation, invasion, adhesion, angiogenesis, trafficking	15	*TMEM14A, MMP14, PIK3R6, ENG, RABL2A, DEPDC1B, TRIM35, CAB39L, AP5S1*	*TSPAN4, SERPINI1, NRP2, RAPGEFL1, FAM195A, AP4M1*	27	*TSPAN2, ARAP3, ITGAM,RARRES3, ADGRE5, FGL2, DYSF, NINI1, ZFP91-CNTF, DENND6B, BGLAP, DOCK3, RNF165, TAX1BP3, TRIM35, TAGLN2, RGS3*	*ADGRG1, TMPRSS6, CYGB, C8orf44-SGK3, LZTS3, MARCKSL1, NACAD, TCF7L2, PHOSPHO2-KLH23, P2RY11*
Immune function	3	*LXN, MTCP1, RSAD2*		4	*SERPINB1, LGALS9, RELT*	*RSAD2*
Metabolism and lipogenesis	17	*ACOT1, ACSF2, CCBL1, MTHFD2L, PPP1R3F, AMPD3, GRHPR*	*PM20D2, TKFC, KDELC1, BDH2, GMPR, BCKDHB, NBR2, NPR2, ENPP1, NR2F6*	7	*TMEM56-RWDD3, SARDH, CYP1A1, GDPGP1, ACSL1, GDE1, ADA*	
Genetic	10	*CBX8, DNAJC30, RPA3, EXOSC7, PPFIBP1*	*TUT1, GTPBP3, MIR600HG, TCEANC, TYRO3P*	9	*TFEC, WWC2, ZBTB7A, HIC1, EFL1, HNRNPLL,TRAK1, CREG1*	*BHLHB9*
Ion transport	1	*SLC35E3*		2	*SLC31A1*	*SLC22A1*
Unknown function	10	*LOC101929767, TTC32, LOC100287042, PROB1*	*ARMCX4, LOC441666, LOC100506804, PRRG4, CBWD6, THAP8*	8	*ZSWIM5, LOC101928464, TNRC6C-AS1, POMGNT2, PLEKho2, NARS2, INTS6L*	*C1QTNF3-AMACR*
Anti-sense, non-coding, snoRNAs	11	*BRWD1-IT2, SNORA67, SNORA17B, LOC100129083, ADNP-AS1, RPL13P5*	*C22orf34, SNHG25, TRIM47, MRPL42P5, GCSHP3*	6	*SNORA17A, SIGLEC17P, NPPA-As1*	*CCDC102A, ALMS1-ITI, LOC100505771*

Supplemental Dataset 1 Pathway analysis of differential gene expression in CK

Summary of WikiPathways data-base analysis for CK uNK versus CK pNK. Frequency of significant differentially-expressed genes (p-value <0.05, Z-Score >1.96), based on Z score.

Criterion: ([LogFC CK uNK vs CK pNK] < -0.26 OR [LogFC CK uNK vs CK pNK] > 0.26) AND [P-value [LogFC CK uNK vs CK pNK] < 0.05

Pathway	positive	measured	total	%	Z Score	p-value
HIF1A and PPARG regulation of glycolysis	6	6	19	100.00%	3.64	0
TGF-beta Signaling Pathway	51	111	133	45.95%	3.38	0.003
Cori Cycle	8	10	53	80.00%	3.33	0
Gastric Cancer Network 1	14	22	30	63.64%	3.29	0.001
Retinoblastoma Gene in Cancer	38	80	98	47.50%	3.16	0.001
Extracellular vesicle-mediated signaling in recipient cells	12	19	31	63.16%	3.01	0
Regulation of sister chromatid separation at metaphase-anaphase transition	10	15	16	66.67%	2.96	0.004
Calcium Regulation in the Cardiac Cell	31	65	164	47.69%	2.88	0.003
Primary Focal Segmental Glomerulosclerosis FSGS	20	38	78	52.63%	2.86	0.003
Fluoropyrimidine Activity	13	22	58	59.09%	2.82	0.001
Integrin-mediated Cell Adhesion	30	64	102	46.88%	2.72	0.004
Focal Adhesion	46	108	201	42.59%	2.57	0.014
Chemokine signaling pathway	42	99	172	42.42%	2.42	0.024
Ebola Virus Pathway on Host	39	91	141	42.86%	2.41	0.018
B Cell Receptor Signaling Pathway	36	83	99	43.37%	2.4	0.009
Nanoparticle-mediated activation of receptor signaling	12	22	36	54.55%	2.36	0.016
Lamin A-processing pathway	4	5	8	80.00%	2.35	0.015
Signal Transduction of S1P Receptor	11	20	26	55.00%	2.3	0.022
MFAP5-mediated ovarian cancer cell motility and invasiveness	6	9	18	66.67%	2.29	0.026
Microglia Pathogen Phagocytosis Pathway	15	30	44	50.00%	2.22	0.027
Histone Modifications	27	61	68	44.26%	2.21	0.024
Association Between Physico-Chemical Features and Toxicity Associated Pathways	22	48	78	45.83%	2.19	0.026
Human Thyroid Stimulating Hormone (TSH) signaling pathway	24	54	67	44.44%	2.1	0.032
Mesodermal Commitment Pathway	35	84	154	41.67%	2.08	0.024
Apoptosis-related network due to altered Notch3 in ovarian cancer	20	44	54	45.45%	2.04	0.047
Regulation of Wnt/B-catenin Signaling by Small Molecule Compounds	7	12	33	58.33%	2.03	0.036
T-Cell antigen Receptor (TCR) Signaling Pathway	32	77	93	41.56%	1.97	0.047

Accepted Manuscript published as REP-18-0509.R1. Accepted for publication: 03-Jun-2019

Purine metabolism	6	10	75	60.00%	1.96	0.044
G Protein Signaling Pathways	25	58	97	43.10%	1.96	0.047
EDA Signalling in Hair Follicle Development	3	4	16	75.00%	1.89	0.045
miRNA targets in ECM and membrane receptors	3	4	46	75.00%	1.89	0.055
TCA Cycle Nutrient Utilization and Invasiveness of Ovarian Cancer	3	4	11	75.00%	1.89	0.04
Non-genomic actions of 1,25 dihydroxyvitamin D3	21	48	97	43.75%	1.88	0.062
ErbB Signaling Pathway	28	67	101	41.79%	1.88	0.063
Development and heterogeneity of the ILC family	8	15	33	53.33%	1.85	0.063
Hypothesized Pathways in Pathogenesis of Cardiovascular Disease	8	15	27	53.33%	1.85	0.045
Vitamin D Receptor Pathway	30	73	188	41.10%	1.83	0.07
Glycolysis and Gluconeogenesis	14	30	69	46.67%	1.83	0.067
Pancreatic adenocarcinoma pathway	31	76	97	40.79%	1.81	0.061
T-Cell antigen Receptor (TCR) pathway during Staphylococcus aureus infection	21	49	70	42.86%	1.76	0.08
Phosphodiesterases in neuronal function	9	18	66	50.00%	1.72	0.088
Genotoxicity pathway	23	55	65	41.82%	1.7	0.077
Regulation of Actin Cytoskeleton	34	86	159	39.53%	1.67	0.105
MAPK and NFkB Signalling Pathways Inhibited by Yersinia YopJ	6	11	13	54.55%	1.67	0.073
Inhibition of exosome biogenesis and secretion by Manumycin A in CRPC cells	8	16	19	50.00%	1.62	0.11
Non-small cell lung cancer	22	53	76	41.51%	1.62	0.12
Myometrial Relaxation and Contraction Pathways	33	84	161	39.29%	1.6	0.102
Signaling Pathways in Glioblastoma	28	70	88	40.00%	1.59	0.111
Epithelial to mesenchymal transition in colorectal cancer	29	73	161	39.73%	1.58	0.107
Disorders of Folate Metabolism and Transport	5	9	46	55.56%	1.58	0.108
Ethanol metabolism resulting in production of ROS by CYP2E1	5	9	28	55.56%	1.58	0.111
GPR40 Pathway	5	9	20	55.56%	1.58	0.114
Adipogenesis	30	76	132	39.47%	1.56	0.118
Factors and pathways affecting insulin-like growth factor (IGF1)-Akt signaling	11	24	34	45.83%	1.55	0.131
MAPK Cascade	11	24	33	45.83%	1.55	0.133
IL-3 Signaling Pathway	17	40	50	42.50%	1.54	0.133
Nucleotide Metabolism	9	19	37	47.37%	1.52	0.123
Hypertrophy Model	7	14	21	50.00%	1.52	0.127
TGF-beta Receptor Signaling	15	35	56	42.86%	1.49	0.154
Arrhythmogenic Right Ventricular Cardiomyopathy	12	27	81	44.44%	1.48	0.13

Thyroxine (Thyroid Hormone) Production	1	1	12	100.00%	1.48	0.123
Tyrosine Metabolism	1	1	23	100.00%	1.48	0.137
Bone Morphogenic Protein (BMP) Signalling and Regulation	4	7	13	57.14%	1.48	0.13
NOTCH1 regulation of human endothelial cell calcification	4	7	18	57.14%	1.48	0.155
Heart Development	8	17	48	47.06%	1.41	0.16
ID signaling pathway	6	12	17	50.00%	1.4	0.197
Striated Muscle Contraction Pathway	6	12	39	50.00%	1.4	0.162
miR-517 relationship with ARCN1 and USP1	3	5	7	60.00%	1.39	0.109
Serotonin and anxiety-related events	3	5	16	60.00%	1.39	0.168
Focal Adhesion-PI3K-Akt-mTOR-signaling pathway	55	152	305	36.18%	1.33	0.185
Common Pathways Underlying Drug Addiction	9	20	50	45.00%	1.33	0.186
Rett syndrome causing genes	12	28	60	42.86%	1.33	0.2
EV release from cardiac cells and their functional effects	2	3	17	66.67%	1.32	0.221
Farnesoid X Receptor Pathway	2	3	21	66.67%	1.32	0.173
Osteoblast Signaling	2	3	18	66.67%	1.32	0.175
Oxytocin signaling	2	3	10	66.67%	1.32	0.22
Synthesis and Degradation of Ketone Bodies	2	3	13	66.67%	1.32	0.224
Vitamins A and D - action mechanisms	2	3	14	66.67%	1.32	0.239
RalA downstream regulated genes	5	10	13	50.00%	1.28	0.232
Transcriptional cascade regulating adipogenesis	5	10	14	50.00%	1.28	0.222
DNA Damage Response (only ATM dependent)	33	88	118	37.50%	1.28	0.201
T-Cell Receptor and Co-stimulatory Signaling	10	23	45	43.48%	1.27	0.187
Type 2 papillary renal cell carcinoma	10	23	41	43.48%	1.27	0.192
Sudden Infant Death Syndrome (SIDS) Susceptibility Pathways	28	74	182	37.84%	1.23	0.204
BDNF-TrkB Signaling	11	26	38	42.31%	1.22	0.213
Fatty Acid Biosynthesis	8	18	37	44.44%	1.21	0.223
Physiological and Pathological Hypertrophy of the Heart	8	18	27	44.44%	1.21	0.24
Hair Follicle Development: Cytodifferentiation (Part 3 of 3)	12	29	92	41.38%	1.18	0.189
Signaling of Hepatocyte Growth Factor Receptor	12	29	35	41.38%	1.18	0.265
TYROBP Causal Network	17	43	61	39.53%	1.18	0.252
Cell Cycle	38	104	124	36.54%	1.18	0.257
Canonical and Non-Canonical TGF-B signaling	6	13	18	46.15%	1.16	0.204
Melatonin metabolism and effects	9	21	64	42.86%	1.15	0.247

Accepted Manuscript published as REP-18-0509.R1. Accepted for publication: 03-Jun-2019

Sphingolipid pathway	9	21	64	42.86%	1.15	0.249
Osteoclast Signaling	4	8	21	50.00%	1.15	0.235
Serotonin and anxiety	4	8	22	50.00%	1.15	0.226
Pathways Affected in Adenoid Cystic Carcinoma	20	52	72	38.46%	1.13	0.251
Alzheimers Disease	21	55	166	38.18%	1.12	0.284
Metabolic reprogramming in colon cancer	15	38	81	39.47%	1.1	0.307
EGF/EGFR Signaling Pathway	49	138	163	35.51%	1.1	0.287
Canonical and Non-canonical Notch signaling	7	16	31	43.75%	1.08	0.294
Wnt Signaling Pathway	16	41	52	39.02%	1.08	0.318
Endochondral Ossification	11	27	69	40.74%	1.07	0.307
Endoderm Differentiation	33	91	147	36.26%	1.04	0.286
Bladder Cancer	12	30	47	40.00%	1.04	0.278
Prostaglandin Synthesis and Regulation	8	19	61	42.11%	1.02	0.274
Vitamin D in inflammatory diseases	8	19	25	42.11%	1.02	0.304
Osteopontin Signaling	5	11	14	45.45%	1.02	0.269
TGF-B Signaling in Thyroid Cells for Epithelial-Mesenchymal Transition	5	11	20	45.45%	1.02	0.283
Pathways in clear cell renal cell carcinoma	22	59	92	37.29%	1.01	0.308
Caloric restriction and aging	3	6	13	50.00%	0.99	0.297
Mammary gland development pathway - Embryonic development (Stage 1 of 4)	3	6	21	50.00%	0.99	0.299
Nicotine Activity on Dopaminergic Neurons	3	6	31	50.00%	0.99	0.308
Alpha 6 Beta 4 signaling pathway	9	22	34	40.91%	0.98	0.329
The effect of progerin on the involved genes in Hutchinson-Gilford Progeria Syndrome	10	25	29	40.00%	0.95	0.352
miRNAs involved in DNA damage response	6	14	70	42.86%	0.94	0.326
Serotonin Receptor 2 and ELK-SRF/GATA4 signaling	6	14	24	42.86%	0.94	0.359
ESC Pluripotency Pathways	19	51	123	37.25%	0.93	0.336
IL-4 Signaling Pathway	19	51	56	37.25%	0.93	0.356
G1 to S cell cycle control	20	54	66	37.04%	0.92	0.348
Corticotropin-releasing hormone signaling pathway	22	60	98	36.67%	0.91	0.347
Chromosomal and microsatellite instability in colorectal cancer	23	63	81	36.51%	0.91	0.346
Prolactin Signaling Pathway	25	69	79	36.23%	0.9	0.355
G13 Signaling Pathway	12	31	39	38.71%	0.9	0.37
Brain-Derived Neurotrophic Factor (BDNF) signaling pathway	36	102	150	35.29%	0.89	0.384
GPCRs, Other	7	17	118	41.18%	0.89	0.379

GPCRs, Class A Rhodopsin-like	14	37	272	37.84%	0.87	0.426
Vitamin A and Carotenoid Metabolism	4	9	65	44.44%	0.86	0.383
One Carbon Metabolism	8	20	57	40.00%	0.85	0.384
Tryptophan metabolism	8	20	133	40.00%	0.85	0.418
Endometrial cancer	18	49	75	36.73%	0.83	0.426
Kit receptor signaling pathway	18	49	60	36.73%	0.83	0.405
RAC1/PAK1/p38/MMP2 Pathway	18	49	74	36.73%	0.83	0.407
AMP-activated Protein Kinase (AMPK) Signaling	19	52	78	36.54%	0.83	0.382
DNA IR-damage and cellular response via ATR	25	70	90	35.71%	0.81	0.407
Cell-type Dependent Selectivity of CCK2R Signaling	2	4	26	50.00%	0.81	0.415
miR-222 in Exercise-Induced Cardiac Growth	2	4	5	50.00%	0.81	0.422
Phase I biotransformations, non P450	2	4	13	50.00%	0.81	0.409
Vitamin D Metabolism	2	4	21	50.00%	0.81	0.407
Angiogenesis	5	12	25	41.67%	0.78	0.403
Neovascularisation processes	5	12	25	41.67%	0.78	0.413
Initiation of transcription and translation elongation at the HIV-1 LTR	11	29	35	37.93%	0.78	0.447
PDGF Pathway	13	35	52	37.14%	0.76	0.447
Endothelin Pathways	6	15	48	40.00%	0.73	0.476
TP53 Network	6	15	23	40.00%	0.73	0.476
Nuclear Receptors	7	18	44	38.89%	0.7	0.471
The human immune response to tuberculosis	7	18	24	38.89%	0.7	0.512
miRs in Muscle Cell Differentiation	8	21	42	38.10%	0.68	0.511
Cell Differentiation - Index	3	7	56	42.86%	0.66	0.525
Differentiation of white and brown adipocyte	3	7	26	42.86%	0.66	0.52
Ganglio Sphingolipid Metabolism	3	7	39	42.86%	0.66	0.527
Hedgehog Signaling Pathway	3	7	17	42.86%	0.66	0.512
Valproic acid pathway	3	7	36	42.86%	0.66	0.503
Nucleotide-binding Oligomerization Domain (NOD) pathway	11	30	43	36.67%	0.64	0.554
Hepatitis C and Hepatocellular Carcinoma	13	36	63	36.11%	0.63	0.552
Exercise-induced Circadian Regulation	14	39	49	35.90%	0.63	0.525
Cardiac Progenitor Differentiation	4	10	56	40.00%	0.6	0.55
Eicosanoid Synthesis	4	10	57	40.00%	0.6	0.548
Aflatoxin B1 metabolism	1	2	16	50.00%	0.57	0.566

Accepted Manuscript published as REP-18-0509.R1. Accepted for publication: 03-Jun-2019

Blood Clotting Cascade	1	2	27	50.00%	0.57	0.588
Hypothetical Craniofacial Development Pathway	1	2	11	50.00%	0.57	0.562
Hypoxia-mediated EMT and Stemness	1	2	6	50.00%	0.57	0.612
miR-509-3p alteration of YAP1/ECM axis	1	2	19	50.00%	0.57	0.607
Ultraconserved region 339 modulation of tumor suppressor microRNAs in cancer	1	2	6	50.00%	0.57	0.618
TNF alpha Signaling Pathway	28	82	97	34.15%	0.57	0.571
Circadian rhythm related genes	41	122	210	33.61%	0.57	0.565
Simplified Interaction Map Between LOXL4 and Oxidative Stress Pathway	5	13	19	38.46%	0.56	0.591
Transcription factor regulation in adipogenesis	5	13	24	38.46%	0.56	0.595
Type II diabetes mellitus	5	13	28	38.46%	0.56	0.59
Wnt Signaling	22	64	121	34.38%	0.54	0.58
4-hydroxytamoxifen, Dexamethasone, and Retinoic Acids Regulation of p27 Expression	6	16	31	37.50%	0.54	0.602
Imatinib and Chronic Myeloid Leukemia	6	16	25	37.50%	0.54	0.62
Interactome of polycomb repressive complex 2 (PRC2)	6	16	17	37.50%	0.54	0.624
MicroRNAs in cardiomyocyte hypertrophy	20	58	109	34.48%	0.54	0.59
Ethanol effects on histone modifications	7	19	53	36.84%	0.53	0.579
Synaptic Vesicle Pathway	7	19	59	36.84%	0.53	0.603
Trans-sulfuration and one carbon metabolism	9	25	66	36.00%	0.51	0.59
Regulation of Microtubule Cytoskeleton	13	37	47	35.14%	0.51	0.655
PI3K-AKT-mTOR signaling pathway and therapeutic opportunities	10	28	33	35.71%	0.51	0.635
Ras Signaling	38	114	192	33.33%	0.49	0.604
GPCRs, Class B Secretin-like	2	5	24	40.00%	0.42	0.63
Liver X Receptor Pathway	2	5	12	40.00%	0.42	0.655
LncRNA-mediated mechanisms of therapeutic resistance	2	5	14	40.00%	0.42	0.667
Macrophage markers	2	5	10	40.00%	0.42	0.668
Role of Osx and miRNAs in tooth development	2	5	39	40.00%	0.42	0.67
RANKL/RANK (Receptor activator of NFKB (ligand)) Signaling Pathway	16	47	58	34.04%	0.42	0.673
Cardiac Hypertrophic Response	14	41	61	34.15%	0.4	0.642
IL-5 Signaling Pathway	12	35	41	34.29%	0.39	0.674
Neural Crest Differentiation	12	35	102	34.29%	0.39	0.697
Target Of Rapamycin (TOR) Signaling	11	32	40	34.38%	0.38	0.666
BMP Signaling Pathway in Eyelid Development	3	8	23	37.50%	0.38	0.697
DNA Mismatch Repair	3	8	10	37.50%	0.38	0.744

Globo Sphingolipid Metabolism	3	8	29	37.50%	0.38	0.664
Cell Differentiation - Index expanded	4	11	69	36.36%	0.37	0.738
H19 action Rb-E2F1 signaling and CDK-Beta-catenin activity	4	11	17	36.36%	0.37	0.784
Cannabinoid receptor signaling	6	17	54	35.29%	0.36	0.712
Pyrimidine metabolism	24	73	140	32.88%	0.3	0.745
Resistin as a regulator of inflammation	8	24	34	33.33%	0.22	0.8
Follicle Stimulating Hormone (FSH) signaling pathway	7	21	28	33.33%	0.21	0.846
IL17 signaling pathway	7	21	32	33.33%	0.21	0.823
Splicing factor NOVA regulated synaptic proteins	7	21	44	33.33%	0.21	0.813
Leptin signaling pathway	21	65	77	32.31%	0.19	0.855
IL-9 Signaling Pathway	5	15	18	33.33%	0.18	0.806
Ovarian Infertility Genes	5	15	33	33.33%	0.18	0.825
Wnt Signaling in Kidney Disease	5	15	39	33.33%	0.18	0.846
VEGFA-VEGFR2 Signaling Pathway	56	176	238	31.82%	0.17	0.879
Pathogenic Escherichia coli infection	12	37	79	32.43%	0.16	0.875
Amplification and Expansion of Oncogenic Pathways as Metastatic Traits	4	12	18	33.33%	0.16	0.849
Development of pulmonary dendritic cells and macrophage subsets	4	12	14	33.33%	0.16	0.825
Androgen receptor signaling pathway	25	78	90	32.05%	0.16	0.882
Extracellular vesicles in the crosstalk of cardiac cells	3	9	30	33.33%	0.14	0.903
NAD metabolism, sirtuins and aging	3	9	16	33.33%	0.14	0.884
SRF and miRs in Smooth Muscle Differentiation and Proliferation	3	9	18	33.33%	0.14	0.886
PI3K-Akt Signaling Pathway	51	161	359	31.68%	0.12	0.879
Alanine and aspartate metabolism	2	6	66	33.33%	0.11	0.902
Cytokines and Inflammatory Response	2	6	32	33.33%	0.11	0.922
Degradation pathway of sphingolipids, including diseases	2	6	38	33.33%	0.11	0.938
exRNA mechanism of action and biogenesis	2	6	8	33.33%	0.11	0.848
Glucuronidation	2	6	41	33.33%	0.11	0.925
Insulin signalling in human adipocytes (diabetic condition)	2	6	12	33.33%	0.11	0.873
Insulin signalling in human adipocytes (normal condition)	2	6	16	33.33%	0.11	0.902
Methionine metabolism leading to Sulphur Amino Acids and related disorders	2	6	41	33.33%	0.11	0.911
miRNA Biogenesis	2	6	7	33.33%	0.11	0.828
Pyrimidine metabolism and related diseases	2	6	51	33.33%	0.11	0.919
Somatroph axis (GH) and its relationship to dietary restriction and aging	2	6	12	33.33%	0.11	0.889

Accepted Manuscript published as REP-18-0509.R1. Accepted for publication: 03-Jun-2019

Type III interferon signaling	2	6	11	33.33%	0.11	0.881
Breast cancer pathway	27	85	167	31.76%	0.11	0.92
Fatty Acid Beta Oxidation	9	28	71	32.14%	0.1	0.909
Arachidonate Epoxygenase / Epoxide Hydrolase	1	3	18	33.33%	0.08	0.987
FTO Obesity Variant Mechanism	1	3	11	33.33%	0.08	0.913
Hfe effect on hepcidin production	1	3	8	33.33%	0.08	0.856
Irinotecan Pathway	1	3	18	33.33%	0.08	0.992
let-7 inhibition of ES cell reprogramming	1	3	17	33.33%	0.08	0.986
Monoamine GPCRs	1	3	43	33.33%	0.08	0.925
Nucleotide GPCRs	1	3	15	33.33%	0.08	0.974
Serotonin Receptor 2 and STAT3 Signaling	1	3	6	33.33%	0.08	0.856
Tgif disruption of Shh signaling	1	3	10	33.33%	0.08	0.905
Vitamin B6-dependent and responsive disorders	1	3	28	33.33%	0.08	0.955
EPO Receptor Signaling	7	22	27	31.82%	0.06	0.974
Hematopoietic Stem Cell Gene Regulation by GABP alpha/beta Complex	6	19	26	31.58%	0.03	0.995
IL-1 signaling pathway	16	51	57	31.37%	0.02	0.994
DNA IR-Double Strand Breaks (DSBs) and cellular response via ATM	15	48	65	31.25%	0	0.993
Notch Signaling Pathway	14	45	62	31.11%	-0.02	0.993
PPAR signaling pathway	9	29	76	31.03%	-0.02	0.964
Prader-Willi and Angelman Syndrome	9	29	90	31.03%	-0.02	0.986
Prion disease pathway	9	29	36	31.03%	-0.02	0.981
IL-2 Signaling Pathway	12	39	43	30.77%	-0.06	0.938
IL-7 Signaling Pathway	7	23	26	30.43%	-0.08	0.965
Tumor suppressor activity of SMARCB1	7	23	35	30.43%	-0.08	0.938
Cysteine and methionine catabolism	3	10	55	30.00%	-0.08	0.894
Glutathione metabolism	3	10	57	30.00%	-0.08	0.92
Nanoparticle triggered regulated necrosis	3	10	25	30.00%	-0.08	0.931
ncRNAs involved in STAT3 signaling in hepatocellular carcinoma	3	10	19	30.00%	-0.08	0.955
Overview of nanoparticle effects	3	10	41	30.00%	-0.08	0.926
Peptide GPCRs	3	10	79	30.00%	-0.08	0.938
Urea cycle and metabolism of amino groups	3	10	71	30.00%	-0.08	0.915
Wnt Signaling Pathway and Pluripotency	19	62	106	30.65%	-0.1	0.909
EBV LMP1 signaling	6	20	25	30.00%	-0.12	0.915

Disorders of the Krebs cycle	2	7	35	28.57%	-0.15	0.926
Matrix Metalloproteinases	2	7	31	28.57%	-0.15	0.906
Supression of HMGB1 mediated inflammation by THBD	2	7	10	28.57%	-0.15	0.859
Integrated Cancer Pathway	12	40	50	30.00%	-0.17	0.852
Interleukin-11 Signaling Pathway	11	37	45	29.73%	-0.2	0.853
MECP2 and Associated Rett Syndrome	11	37	101	29.73%	-0.2	0.828
TNF related weak inducer of apoptosis (TWEAK) Signaling Pathway	11	37	45	29.73%	-0.2	0.841
Gastric Cancer Network 2	7	24	33	29.17%	-0.22	0.799
One carbon metabolism and related pathways	9	31	94	29.03%	-0.27	0.791
Acetylcholine Synthesis	1	4	18	25.00%	-0.27	0.781
BMP2-WNT4-FOXO1 Pathway in Human Primary Endometrial Stromal Cell Differentiation	1	4	16	25.00%	-0.27	0.79
Drug Induction of Bile Acid Pathway	1	4	45	25.00%	-0.27	0.773
Methylation Pathways	1	4	15	25.00%	-0.27	0.782
MicroRNA for Targeting Cancer Growth and Vascularization in Glioblastoma	1	4	10	25.00%	-0.27	0.736
Molybdenum cofactor (Moco) biosynthesis	1	4	20	25.00%	-0.27	0.776
Oligodendrocyte Specification and differentiation(including remyelination), leading to Myelin C	1	4	46	25.00%	-0.27	0.788
PTF1A related regulatory pathway	1	4	12	25.00%	-0.27	0.783
Energy Metabolism	12	41	49	29.27%	-0.27	0.763
Thymic Stromal LymphoPoietin (TSLP) Signaling Pathway	12	41	49	29.27%	-0.27	0.764
Differentiation Pathway	3	11	64	27.27%	-0.28	0.76
Monoamine Transport	3	11	47	27.27%	-0.28	0.796
miRNA Regulation of DNA Damage Response	18	61	106	29.51%	-0.29	0.797
NRF2 pathway	18	61	145	29.51%	-0.29	0.768
DNA Damage Response	17	58	76	29.31%	-0.32	0.734
Aryl Hydrocarbon Receptor	10	35	57	28.57%	-0.34	0.761
Ectoderm Differentiation	22	75	145	29.33%	-0.36	0.688
ERK Pathway in Huntington's Disease	2	8	16	25.00%	-0.38	0.713
Iron metabolism in placenta	2	8	15	25.00%	-0.38	0.75
NLR Proteins	2	8	11	25.00%	-0.38	0.723
Small Ligand GPCRs	2	8	25	25.00%	-0.38	0.688
Notch Signaling	9	32	48	28.13%	-0.38	0.668
Methionine De Novo and Salvage Pathway	4	15	74	26.67%	-0.38	0.709
TCA Cycle and Deficiency of Pyruvate Dehydrogenase complex (PDHc)	4	15	37	26.67%	-0.38	0.686

Accepted Manuscript published as REP-18-0509.R1. Accepted for publication: 03-Jun-2019

Lung fibrosis	6	22	85	27.27%	-0.4	0.675
White fat cell differentiation	6	22	35	27.27%	-0.4	0.68
Metapathway biotransformation Phase I and II	14	49	191	28.57%	-0.4	0.694
Triacylglyceride Synthesis	3	12	37	25.00%	-0.47	0.63
Type II interferon signaling (IFNG)	7	26	38	26.92%	-0.48	0.633
Glycogen Synthesis and Degradation	9	33	54	27.27%	-0.49	0.66
Interferon type I signaling pathways	14	50	57	28.00%	-0.5	0.632
Mammary gland development pathway - Pregnancy and lactation (Stage 3 of 4)	4	16	42	25.00%	-0.54	0.598
MTHFR deficiency	4	16	54	25.00%	-0.54	0.569
Serotonin Receptor 4/6/7 and NR3C Signaling	4	16	22	25.00%	-0.54	0.611
Wnt/beta-catenin Signaling Pathway in Leukemia	4	16	29	25.00%	-0.54	0.635
Benzo(a)pyrene metabolism	1	5	17	20.00%	-0.54	0.628
Genes targeted by miRNAs in adipocytes	1	5	19	20.00%	-0.54	0.587
Metabolism of Spingolipids in ER and Golgi apparatus	1	5	69	20.00%	-0.54	0.564
mir-124 predicted interactions with cell cycle and differentiation	1	5	8	20.00%	-0.54	0.641
Oncostatin M Signaling Pathway	15	54	66	27.78%	-0.55	0.581
Angiopoietin Like Protein 8 Regulatory Pathway	29	101	156	28.71%	-0.55	0.574
Structural Pathway of Interleukin 1 (IL-1)	12	44	52	27.27%	-0.57	0.546
Mammary gland development pathway - Puberty (Stage 2 of 4)	2	9	15	22.22%	-0.58	0.554
Trans-sulfuration pathway	2	9	25	22.22%	-0.58	0.548
Insulin Signaling	39	135	162	28.89%	-0.6	0.536
Oxidative Damage	7	27	44	25.93%	-0.6	0.575
MAPK Signaling Pathway	45	155	259	29.03%	-0.6	0.571
Phytochemical activity on NRF2 transcriptional activation	3	13	20	23.08%	-0.64	0.539
PI3K/AKT/mTOR - VitD3 Signalling	3	13	34	23.08%	-0.64	0.532
IL-6 signaling pathway	10	38	45	26.32%	-0.66	0.526
Aryl Hydrocarbon Receptor Pathway	6	24	49	25.00%	-0.66	0.53
Arylamine metabolism	0	1	13	0.00%	-0.67	0.519
Biogenic Amine Synthesis	0	1	33	0.00%	-0.67	0.482
Composition of Lipid Particles	0	1	21	0.00%	-0.67	0.52
Evolocumab Mechanism	0	1	5	0.00%	-0.67	0.476
Fatty Acid Omega Oxidation	0	1	20	0.00%	-0.67	0.493
Heroin metabolism	0	1	8	0.00%	-0.67	0.513

Hormonal control of Pubertal Growth Spurt	0	1	8	0.00%	-0.67	0.492
Influenza A virus infection	0	1	16	0.00%	-0.67	0.506
mir34a and TGIF2 in osteoclastogenesis	0	1	5	0.00%	-0.67	0.457
Model for regulation of MSMP expression in cancer cells and its proangiogenic role in ovariar	0	1	6	0.00%	-0.67	0.493
Proprotein convertase subtilisin/kexin type 9 (PCSK9) mediated LDL receptor degradation	0	1	3	0.00%	-0.67	0.336
SCFA and skeletal muscle substrate metabolism	0	1	17	0.00%	-0.67	0.508
Mitochondrial Gene Expression	4	17	23	23.53%	-0.69	0.488
NAD+ biosynthetic pathways	4	17	37	23.53%	-0.69	0.516
miRNA regulation of p53 pathway in prostate cancer	5	21	37	23.81%	-0.74	0.448
NRF2-ARE regulation	5	21	24	23.81%	-0.74	0.51
ATM Signaling Network in Development and Disease	10	39	49	25.64%	-0.76	0.431
Statin Pathway	2	10	50	20.00%	-0.77	0.463
DDX1 as a regulatory component of the Drosha microprocessor	1	6	8	16.67%	-0.77	0.479
Dual hijack model of Vif in HIV infection	1	6	10	16.67%	-0.77	0.457
Role Altered Glycolysation of MUC1 in Tumour Microenvironment	1	6	10	16.67%	-0.77	0.461
Photodynamic therapy-induced HIF-1 survival signaling	6	25	38	24.00%	-0.78	0.423
Inflammatory Response Pathway	3	14	34	21.43%	-0.79	0.426
Oxidation by Cytochrome P450	3	14	75	21.43%	-0.79	0.444
ncRNAs involved in Wnt signaling in hepatocellular carcinoma	11	43	89	25.58%	-0.8	0.427
TCA Cycle (aka Krebs or citric acid cycle)	4	18	49	22.22%	-0.83	0.411
Fibrin Complement Receptor 3 Signaling Pathway	5	22	44	22.73%	-0.86	0.347
ATM Signaling Pathway	8	33	50	24.24%	-0.87	0.338
Photodynamic therapy-induced unfolded protein response	6	26	28	23.08%	-0.9	0.396
Nuclear Receptors Meta-Pathway	42	151	339	27.81%	-0.92	0.34
Complement and Coagulation Cascades	2	11	63	18.18%	-0.94	0.358
Homologous recombination	2	11	14	18.18%	-0.94	0.402
NAD+ metabolism	2	11	34	18.18%	-0.94	0.372
Mitochondrial LC-Fatty Acid Beta-Oxidation	3	15	24	20.00%	-0.94	0.35
SREBF and miR33 in cholesterol and lipid homeostasis	3	15	19	20.00%	-0.94	0.364
Integrated Breast Cancer Pathway	38	138	201	27.54%	-0.95	0.358
ACE Inhibitor Pathway	0	2	29	0.00%	-0.95	0.347
Benzene metabolism	0	2	17	0.00%	-0.95	0.372
Butyrate-induced histone acetylation	0	2	11	0.00%	-0.95	0.367

Accepted Manuscript published as REP-18-0509.R1. Accepted for publication: 03-Jun-2019

Codeine and Morphine Metabolism	0	2	26	0.00%	-0.95	0.346
Complement Activation	0	2	24	0.00%	-0.95	0.362
Mevalonate arm of cholesterol biosynthesis pathway with inhibitors	0	2	60	0.00%	-0.95	0.349
Polyol Pathway	0	2	17	0.00%	-0.95	0.405
Sulindac Metabolic Pathway	0	2	11	0.00%	-0.95	0.368
Tamoxifen metabolism	0	2	36	0.00%	-0.95	0.357
Non-homologous end joining	1	7	9	14.29%	-0.97	0.336
Thiamine metabolic pathways	1	7	34	14.29%	-0.97	0.322
Amino Acid metabolism	15	59	205	25.42%	-0.97	0.323
Senescence and Autophagy in Cancer	21	80	112	26.25%	-0.97	0.307
Hedgehog Signaling Pathway	5	23	44	21.74%	-0.99	0.326
Toll-like Receptor Signaling	5	23	32	21.74%	-0.99	0.318
Thermogenesis	19	74	140	25.68%	-1.04	0.291
AGE/RAGE pathway	13	53	67	24.53%	-1.06	0.292
Lipid Metabolism Pathway	4	20	43	20.00%	-1.09	0.265
Nanoparticle triggered autophagic cell death	4	20	30	20.00%	-1.09	0.276
Oxidative Stress	4	20	35	20.00%	-1.09	0.274
Leptin Insulin Overlap	2	12	20	16.67%	-1.09	0.278
LncRNA involvement in canonical Wnt signaling and colorectal cancer	12	50	102	24.00%	-1.11	0.245
ATR Signaling	1	8	10	12.50%	-1.14	0.317
GABA receptor Signaling	1	8	57	12.50%	-1.14	0.25
Heme Biosynthesis	1	8	28	12.50%	-1.14	0.272
Mammary gland development pathway - Involution (Stage 4 of 4)	1	8	13	12.50%	-1.14	0.277
Apoptosis Modulation and Signaling	18	72	97	25.00%	-1.15	0.269
Dopaminergic Neurogenesis	0	3	32	0.00%	-1.17	0.231
eIF5A regulation in response to inhibition of the nuclear export system	0	3	6	0.00%	-1.17	0.212
Glial Cell Differentiation	0	3	9	0.00%	-1.17	0.231
Glycine Metabolism	0	3	19	0.00%	-1.17	0.247
Robo4 and VEGF Signaling Pathways Crosstalk	0	3	7	0.00%	-1.17	0.233
Steroid Biosynthesis	0	3	25	0.00%	-1.17	0.226
Spinal Cord Injury	12	51	127	23.53%	-1.19	0.215
DNA Replication	9	40	50	22.50%	-1.2	0.224
miRNAs involvement in the immune response in sepsis	5	25	69	20.00%	-1.22	0.233

Human Complement System	7	33	143	21.21%	-1.25	0.199
Interleukin-1 Induced Activation of NF-kappa-B	1	9	13	11.11%	-1.3	0.247
Photodynamic therapy-induced NF-kB survival signaling	4	22	36	18.18%	-1.32	0.175
Glycerophospholipid Biosynthetic Pathway	3	18	94	16.67%	-1.34	0.175
Photodynamic therapy-induced NFE2L2 (NRF2) survival signaling	3	18	24	16.67%	-1.34	0.205
Zinc homeostasis	3	18	39	16.67%	-1.34	0.18
Ferroptosis	7	34	70	20.59%	-1.34	0.162
Gene regulatory network modelling somitogenesis	0	4	13	0.00%	-1.35	0.18
MicroRNA network associated with chronic lymphocytic leukemia	0	4	10	0.00%	-1.35	0.147
NAD Biosynthesis II (from tryptophan)	0	4	34	0.00%	-1.35	0.219
Peroxisomal beta-oxidation of tetracosanoyl-CoA	0	4	17	0.00%	-1.35	0.186
Toll-like Receptor Signaling Pathway	14	61	110	22.95%	-1.41	0.168
Eukaryotic Transcription Initiation	7	35	42	20.00%	-1.44	0.14
Deregulation of Rab and Rab Effector Genes in Bladder Cancer	1	10	17	10.00%	-1.45	0.15
Kennedy pathway from Sphingolipids	1	10	35	10.00%	-1.45	0.134
Simplified Depiction of MYD88 Distinct Input-Output Pathway	1	10	20	10.00%	-1.45	0.146
Regulation of toll-like receptor signaling pathway	22	91	153	24.18%	-1.47	0.15
IL1 and megakaryocytes in obesity	2	15	26	13.33%	-1.5	0.122
ApoE and miR-146 in inflammation and atherosclerosis	0	5	11	0.00%	-1.51	0.078
Folate-Alcohol and Cancer Pathway Hypotheses	0	5	24	0.00%	-1.51	0.124
Serotonin Transporter Activity	0	5	15	0.00%	-1.51	0.087
Sulfation Biotransformation Reaction	0	5	29	0.00%	-1.51	0.134
Sterol Regulatory Element-Binding Proteins (SREBP) signalling	13	59	77	22.03%	-1.53	0.109
TLR4 Signaling and Tolerance	4	24	30	16.67%	-1.54	0.123
Estrogen signaling pathway	3	20	26	15.00%	-1.57	0.11
NO/cGMP/PKG mediated Neuroprotection	3	20	64	15.00%	-1.57	0.127
Oxidative phosphorylation	10	49	68	20.41%	-1.64	0.104
RIG-I-like Receptor Signaling	10	49	64	20.41%	-1.64	0.1
Estrogen metabolism	0	6	45	0.00%	-1.65	0.128
Leptin and adiponectin	0	6	14	0.00%	-1.65	0.082
Metastatic brain tumor	0	6	28	0.00%	-1.65	0.09
Preimplantation Embryo	3	21	60	14.29%	-1.68	0.081
Fas Ligand (FasL) pathway and Stress induction of Heat Shock Proteins (HSP) regulation	7	38	48	18.42%	-1.71	0.093

Accepted Manuscript published as REP-18-0509.R1. Accepted for publication: 03-Jun-2019

Constitutive Androstane Receptor Pathway	1	12	34	8.33%	-1.71	0.084
Nuclear Receptors in Lipid Metabolism and Toxicity	1	12	48	8.33%	-1.71	0.099
PPAR Alpha Pathway	1	12	28	8.33%	-1.71	0.083
Copper homeostasis	6	34	58	17.65%	-1.72	0.071
Translation Factors	9	46	51	19.57%	-1.72	0.095
Regulation of Apoptosis by Parathyroid Hormone-related Protein	2	17	24	11.76%	-1.74	0.071
Dopamine metabolism	0	7	48	0.00%	-1.78	0.068
Pentose Phosphate Metabolism	0	7	21	0.00%	-1.78	0.064
TFs Regulate miRNAs related to cardiac hypertrophy	0	7	16	0.00%	-1.78	0.056
Folate Metabolism	5	31	139	16.13%	-1.82	0.062
Pregnane X Receptor pathway	1	13	35	7.69%	-1.83	0.079
Viral Acute Myocarditis	11	56	109	19.64%	-1.88	0.066
Estrogen Receptor Pathway	0	8	16	0.00%	-1.91	0.044
p38 MAPK Signaling Pathway	4	28	36	14.29%	-1.94	0.048
Parkinsons Disease Pathway	4	28	84	14.29%	-1.94	0.061
Cholesterol Biosynthesis Pathway	1	14	32	7.14%	-1.95	0.04
Vitamin B12 Disorders	0	9	35	0.00%	-2.02	0.038
Amyotrophic lateral sclerosis (ALS)	4	29	56	13.79%	-2.03	0.042
Mitochondrial complex I assembly model OXPHOS system	8	46	61	17.39%	-2.04	0.042
Nanomaterial induced apoptosis	2	20	30	10.00%	-2.05	0.039
Nonalcoholic fatty liver disease	28	124	170	22.58%	-2.11	0.035
Apoptosis	14	71	88	19.72%	-2.11	0.041
Apoptosis Modulation by HSP70	1	17	22	5.88%	-2.26	0.023
Proteasome Degradation	8	53	67	15.09%	-2.55	0.01
Selenium Metabolism and Selenoproteins	3	31	56	9.68%	-2.6	0.008
Electron Transport Chain (OXPHOS system in mitochondria)	15	83	119	18.07%	-2.61	0.006
Vitamin B12 Metabolism	1	21	118	4.76%	-2.62	0.008
Selenium Micronutrient Network	5	41	195	12.20%	-2.64	0.008
Parkin-Ubiquitin Proteasomal System pathway	8	55	75	14.55%	-2.69	0.005
Allograft Rejection	2	32	113	6.25%	-3.06	0.002
Ciliary landscape	38	185	215	20.54%	-3.2	0.003
mRNA Processing	15	118	130	12.71%	-4.39	0
Cytoplasmic Ribosomal Proteins	3	80	89	3.75%	-5.35	0

Acrylamide Biotransformation and Exposure Biomarkers	0	0	10	NaN%	NaN	0
Amino acid conjugation of benzoic acid	0	0	14	NaN%	NaN	0
Amino acid conjugation	0	0	7	NaN%	NaN	0
Aripiprazole Metabolic Pathway	0	0	7	NaN%	NaN	0
Biochemical Pathways Part I	0	0	471	NaN%	NaN	0
Biosynthesis and regeneration of tetrahydrobiopterin (BH4) and catabolism of phenylalanine,	0	0	31	NaN%	NaN	0
Caffeine and Theobromine metabolism	0	0	17	NaN%	NaN	0
Carnosine's role in mucle contraction	0	0	14	NaN%	NaN	0
Catalytic cycle of mammalian Flavin-containing MonoOxygenases (FMOs)	0	0	14	NaN%	NaN	0
Colchicine Metabolic Pathway	0	0	5	NaN%	NaN	0
Diclofenac Metabolic Pathway	0	0	12	NaN%	NaN	0
Effects of Nitric Oxide	0	0	16	NaN%	NaN	0
FABP4 in ovarian cancer	0	0	3	NaN%	NaN	0
Felbamate Metabolism	0	0	12	NaN%	NaN	0
Gastric acid production	0	0	22	NaN%	NaN	0
GHB metabolic pathway	0	0	25	NaN%	NaN	0
Glucocorticoid and Mineralcorticoid Metabolism	0	0	26	NaN%	NaN	0
Glucose Homeostasis	0	0	24	NaN%	NaN	0
GPCRs, Class C Metabotropic glutamate, pheromone	0	0	15	NaN%	NaN	0
Human metabolism overview	0	0	115	NaN%	NaN	0
Lidocaine metabolism	0	0	11	NaN%	NaN	0
Metabolism of Dichloroethylene by CYP450	0	0	13	NaN%	NaN	0
Metabolism of Tetrahydrocannabinol (THC)	0	0	11	NaN%	NaN	0
Mevalonate arm of cholesterol biosynthesis pathway	0	0	29	NaN%	NaN	0
Modified nucleosides derived from t-RNA as urinary cancer markers	0	0	21	NaN%	NaN	0
Neurotransmitter Disorders	0	0	23	NaN%	NaN	0
Nicotine Activity on Chromaffin Cells	0	0	10	NaN%	NaN	0
Nicotine Metabolism	0	0	18	NaN%	NaN	0
Ophthalmate biosynthesis in hepatocytes	0	0	10	NaN%	NaN	0
Phosphatidylcholine catabolism	0	0	32	NaN%	NaN	0
Secretion of Hydrochloric Acid in Parietal Cells	0	0	15	NaN%	NaN	0

Accepted Manuscript published as REP-18-0509.R1. Accepted for publication: 03-Jun-2019

uNK versus CK pNK

total genes measured as a proportion of the total frequency of pathway enriched genes were ranked

ID	Age	BMI	Ethnicity	Gestation (w)	Smoking status	G/P	Living	Stillbirth	Miscarriage	TOP
40	33	29.4	White British	7+4	N	G5P3 +1	2	0	1	0
41	33	24.5	Black Caribbean	11+2	N	G1P0	0	0	0	0
43	19	22.3	White British	9+4	N	G1P0	0	0	0	0
42	35	22.7	Pakistani	7	Y - 6/day	G4P3	3	0	0	0

Supplemental Table 1. Summary of decidua donor demographic analysis. Data show: Identification number (ID), maternal age, body mass index (BMI), ethnicity, gestational age at surgical termination of pregnancy (sTOP) (w; weeks), smoking status (yes [Y] / no [N] - total / day), gravida and parity (G/P) with obstetric history; living, stillbirth, miscarriage, TOP.

Accepted Manuscript published as REP-18-0509.R1. Accepted for publication: 03-Jun-2019

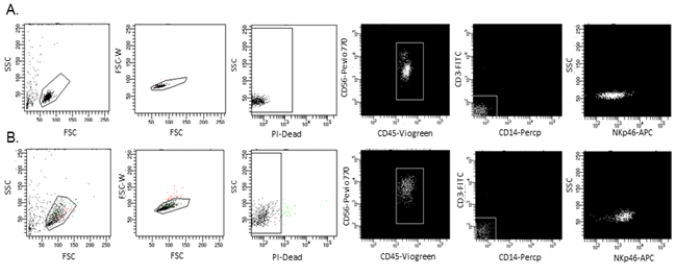

C.

ID	Maternal pNK (%)	Decidua uNK (%)
40	99.1	96.0
41	99.0	98.7
42	99.2	98.5
43	99.0	98.3

Supplemental Figure 1. FACS parameters for isolation of NK cells for RNAseq. Peripheral blood (A) and decidua (B) cell FACS gating strategy. Forward scatter (FSC), side scatter (SSC), pulse width (FSC-W) were used to identify lymphocytes singlets. Propidium iodide (PI)-Dead identified live cells with CD45+ CD56+ NKp46+ cells, negative for CD14 and CD3 subsequently identified for NK cell sorting.

254x190mm (96 x 96 DPI)

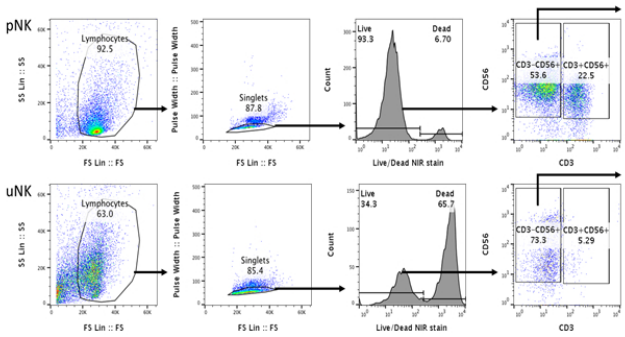

Supplemental Figure 2. Flow cytometry gating strategy VDR and CD69 analysis. Representative flow cytometry plots of the gating strategy utilised to identify live CD3-CD56+ pNK (A) and uNK (B) cells for VDR and CD69 analysis following CD56+ positive selection and 24-hour culture in the presence and absence of cytokine stimulation and active $1,25(OH)_2D3$.

254x190mm (96 x 96 DPI)

Accepted Manuscript published as REP-18-0509.R1. Accepted for publication: 03-Jun-2019

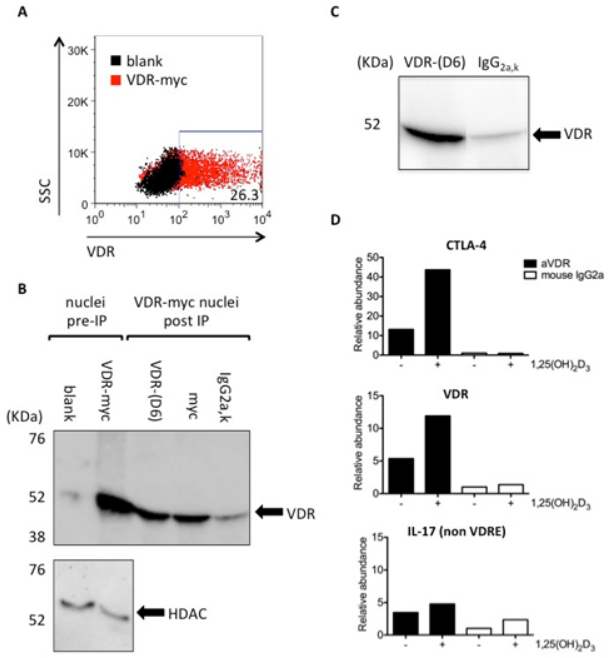

Supplemental Figure 3. Anti-human vitamin D receptor (VDR) antibody (D6 clone) can detect and immunoprecipitate VDR from human T cells. A) VDR expression in non-transfected (black) and VDR-myc-transfected (red) Jurkat T cells as detected by flow cytometry using mouse anti-human VDR (D6) clone (aVDR). B) Immunoprecipitations (IP) with aVDR, anti-myc (amyc) and anti-IgG2a,k (aIgG2a,k) antibodies was performed on nuclei from VDR-myc-transfected Jurkat T cells. Nuclei pre-IP and IP products were immunoblotted with non-competing aVDR (9A7). Histone deacetylase (HDAC) was used as a loading control. C) aVDR (D6) was used to IP VDR from the chromatin fraction of aCD3/CD28-stimulated T cells. IP products were immunoblotted with non-competing aVDR (9A7). D) VDR-chromatin immunoprecipitation (ChIP) with D6 aVDR was performed on $1,25(OH)_2D3$- and vehicle-treated aCD3/CD28-stimulated CD4+ T cells. Relative abundance of VDR on vitamin D response element (VDRE) cDNAs for CTLA-4 and VDR-promoters, and a non-VDRE region of the IL-17 promoter is shown.

190x254mm (96 x 96 DPI)

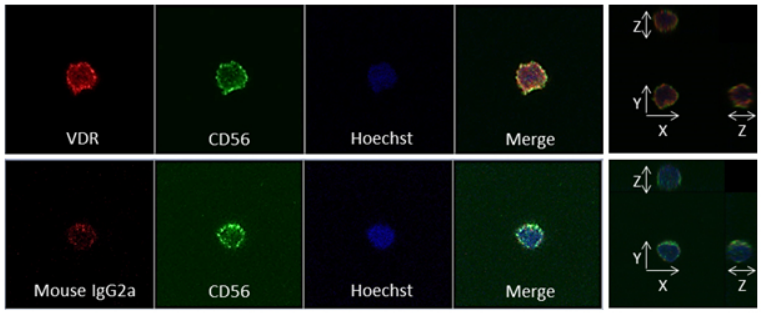

Supplemental Figure 4. Representative Z stack confocal images of VDR expression in CD56+ mononuclear cells from 12 week pregnant mother blood following overnight stimulation with IL-15, IL-12 and IL-2. Left: Single and merge track images. Right: X,Y,Z orthogonal views through the cell.

190x254mm (96 x 96 DPI)

Accepted Manuscript published as REP-18-0509.R1. Accepted for publication: 03-Jun-2019

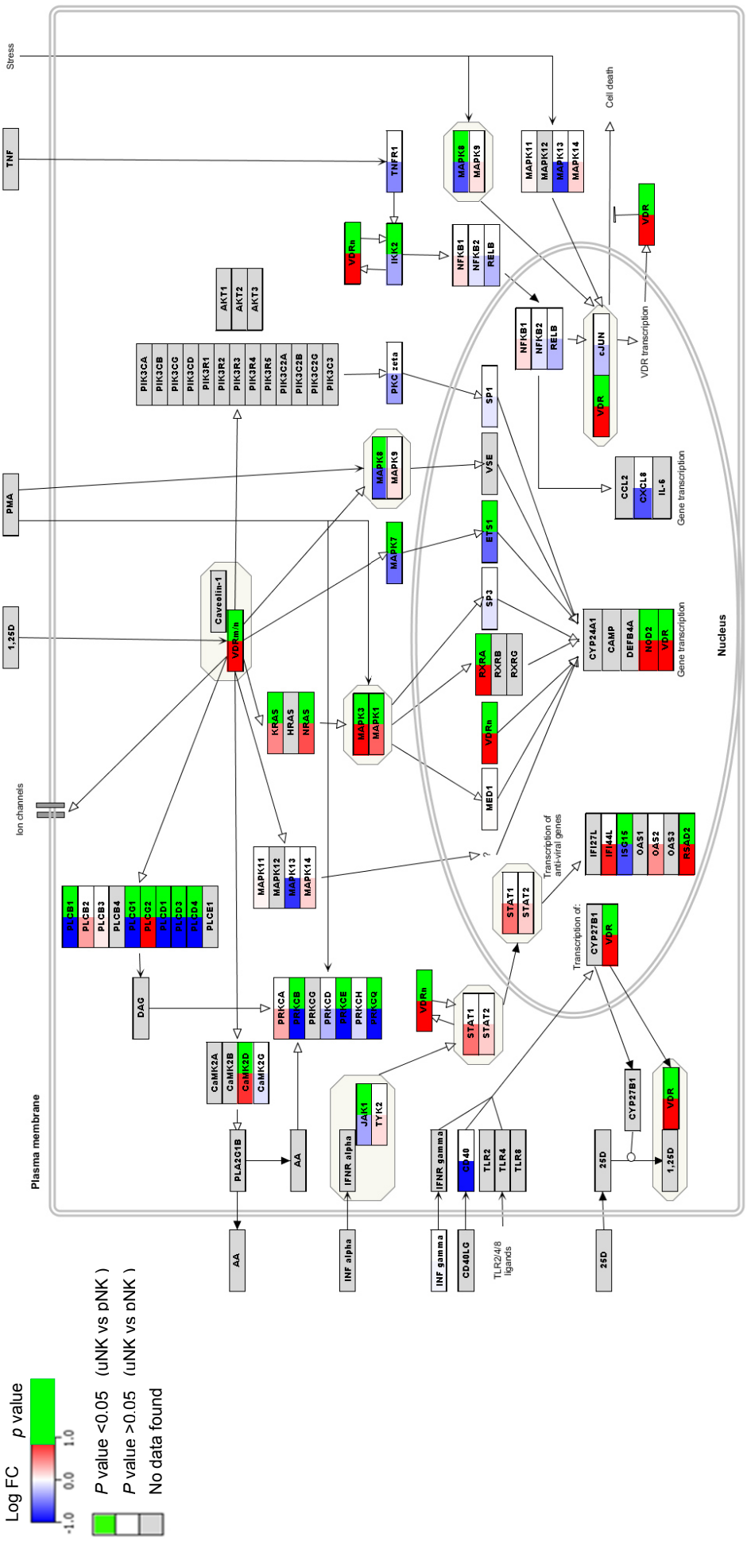

Supplemental Figure 5A. Pathway analysis of genes associated with non-genomic responses to 1,25(OH)$_2$D3 in CK-stimulated uNK versus CK-stimulated pNK. Visualisation of genes with enhanced (red) or suppressed (blue) expression in cytokine-stimulated uNK versus cytokine-stimulated pNK. Individual genes are shown in boxes and box colour split into two parts, (1) the log2 fold-change (Log FC) in the left part of the box (blue down-regulated, white not changed, red up-regulated) and (2) the *p*-value for statistical significance is shown in the right part of the box (green when significant). Pathway elements including genes not assessed in the selected dataset are shown in grey.

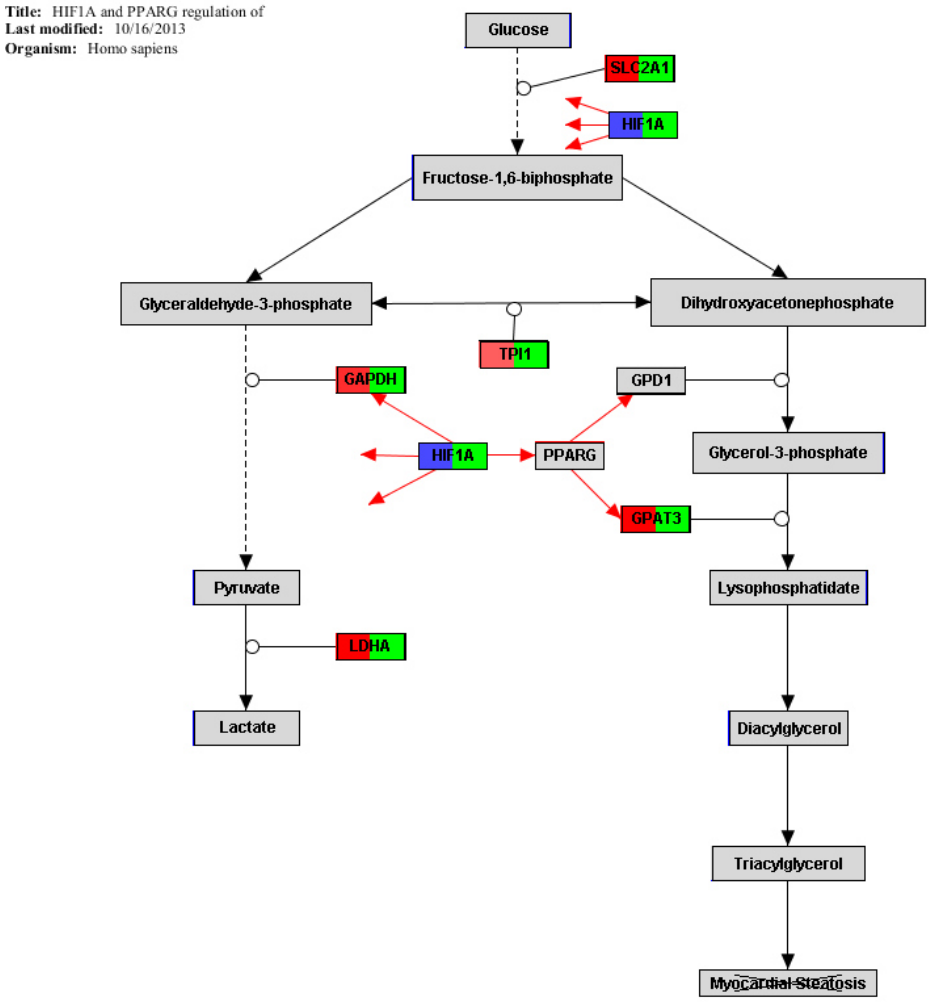

Supplemental Figure 5B. Pathway analysis of HIF1A and PPARG regulation of glycolysis-related genes in CK-stimulated uNK versus CK-stimulated pNK. Visualisation of genes with enhanced (red) or suppressed (blue) expression in cytokine-stimulated uNK versus cytokine-stimulated pNK. Individual genes are shown in boxes and box colour split into two parts, (1) the log2 fold-change in the left part of the box (blue down-regulated, white not changed, red up-regulated) and (2) the *p*-value for statistical significance is shown in the right part of the box (green when significant). Pathway elements including genes not assessed in the selected dataset are shown in grey.

Accepted Manuscript published as REP-18-0509.R1. Accepted for publication: 03-Jun-2019

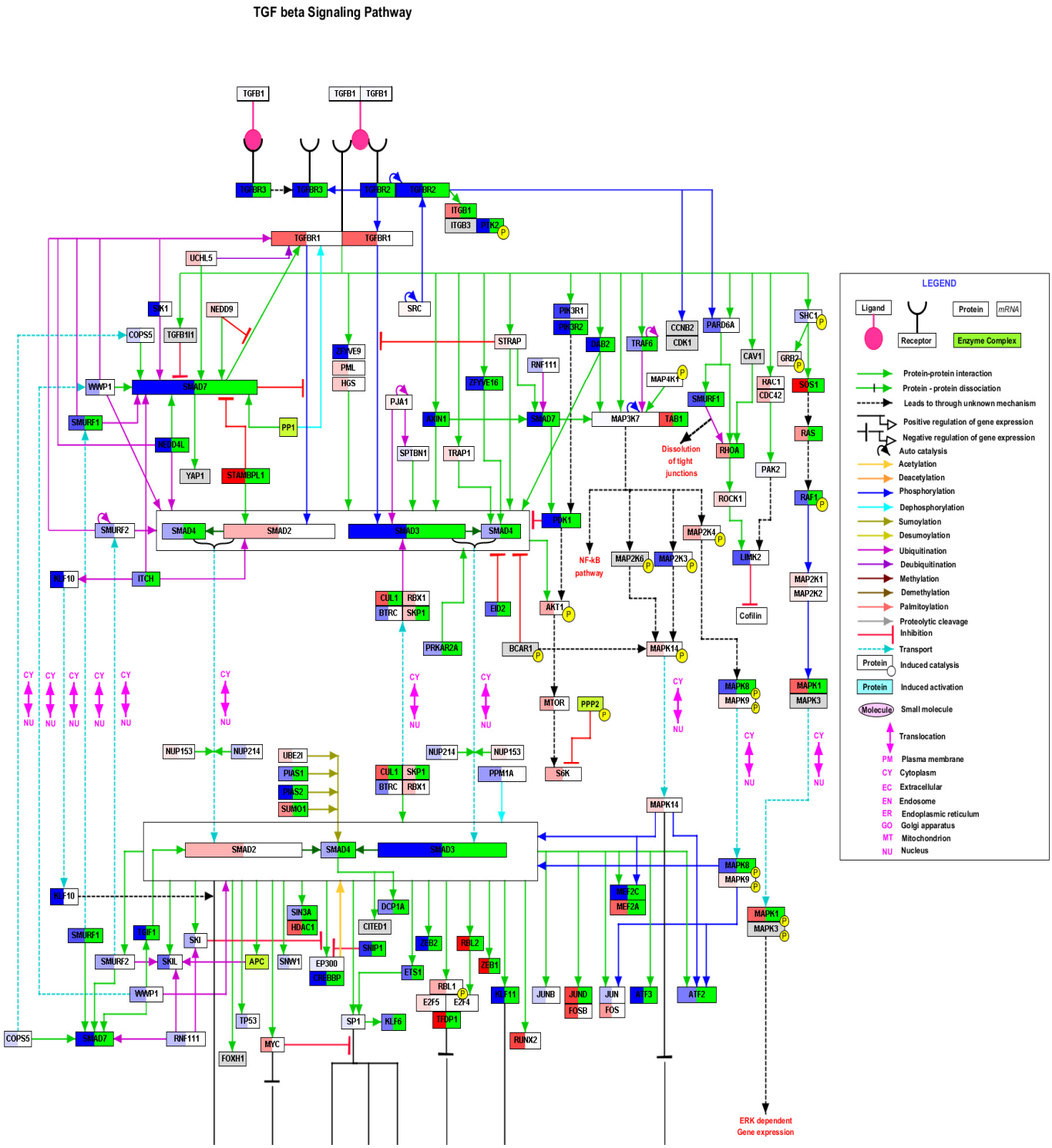

Supplemental Figure 5C. Pathway analysis of TGFβ signalling pathway in CK-stimulated uNK versus CK-stimulated pNK.

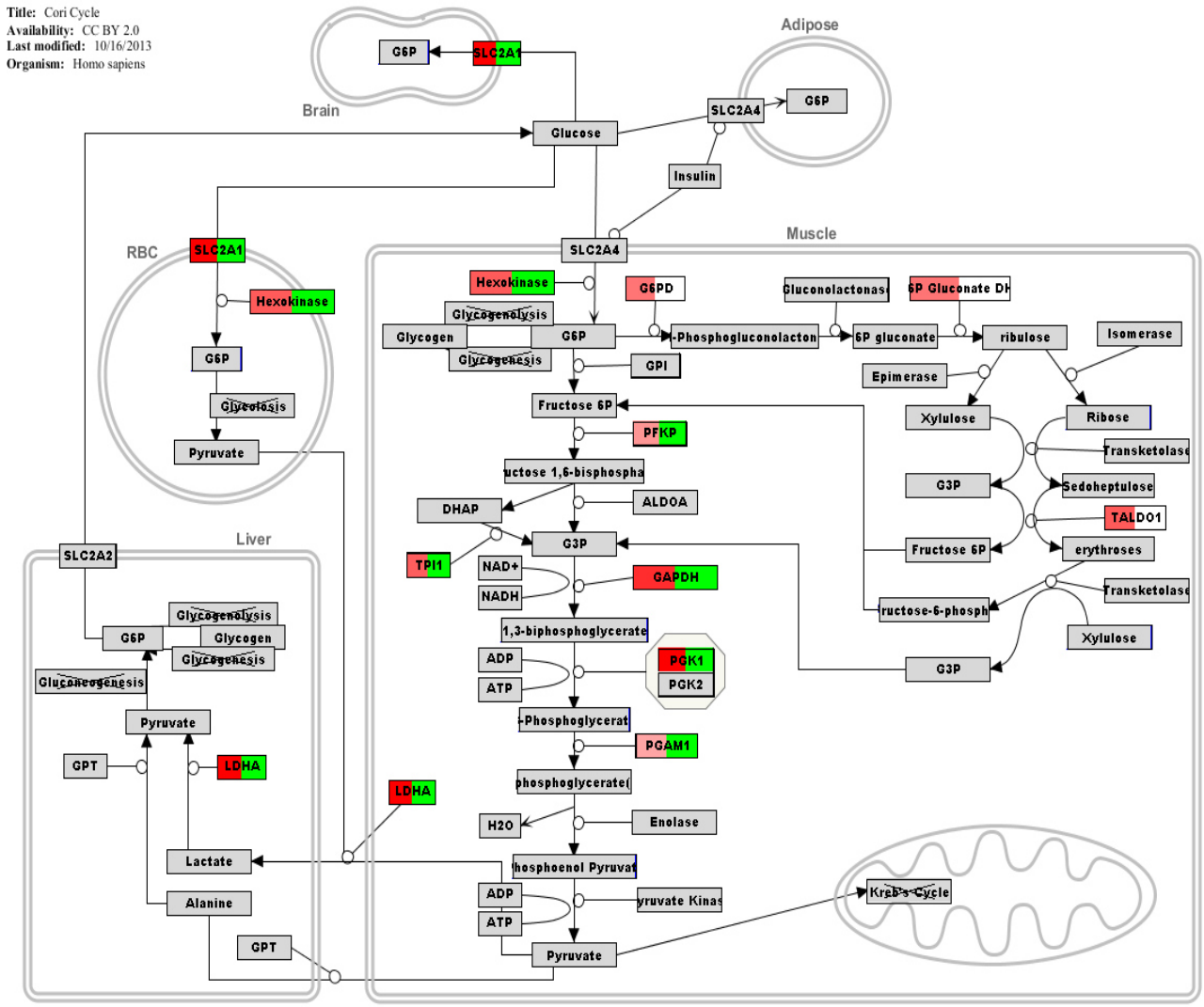

Supplemental Figure 5D. Pathway analysis of the Cori cycle in CK-stimulated uNK versus CK-stimulated pNK.

Accepted Manuscript published as REP-18-0509.R1. Accepted for publication: 03-Jun-2019

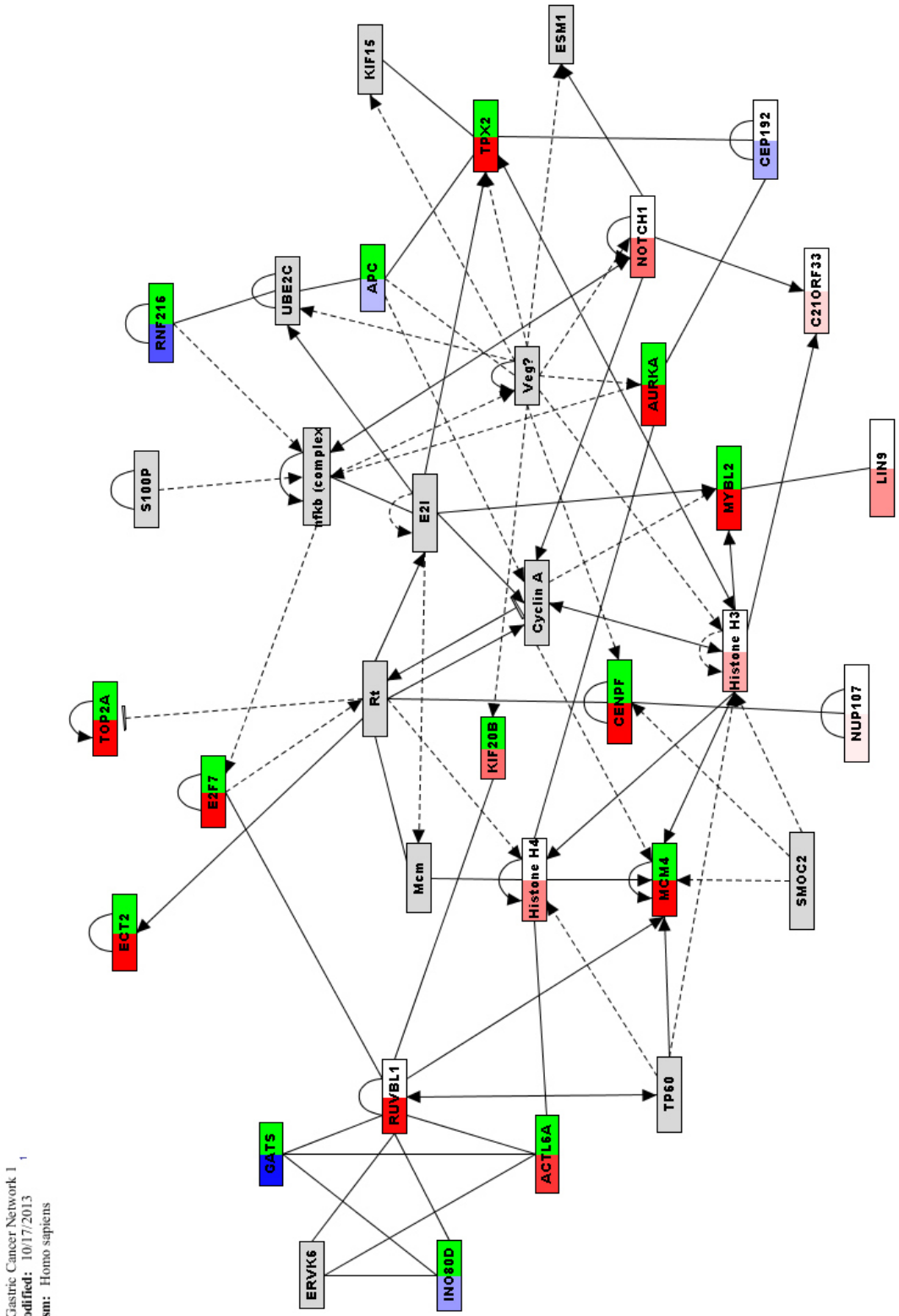

Supplemental Figure 5E. Pathway analysis of the gastric cancer network in CK-stimulated uNK versus CK-stimulated pNK.

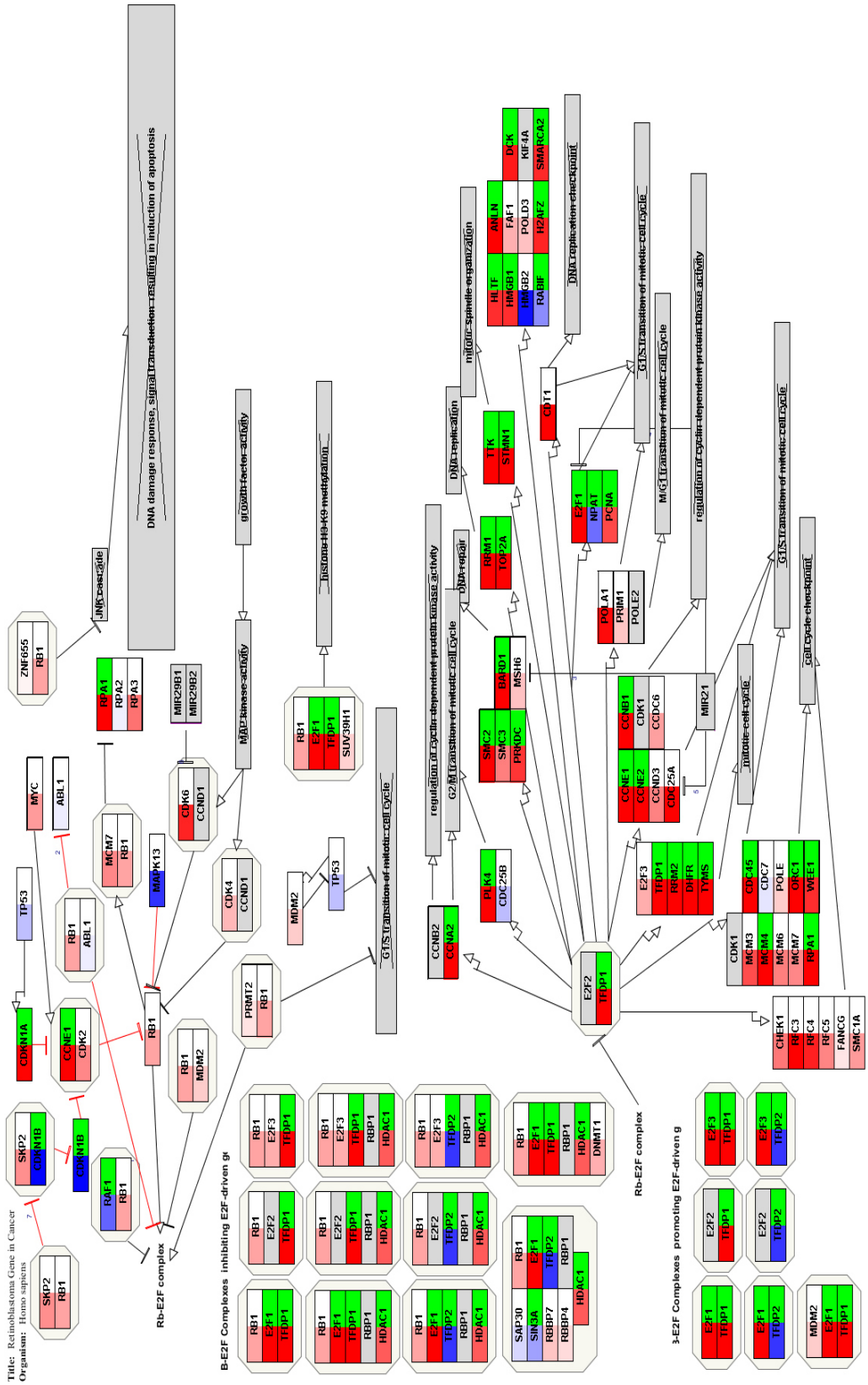

Supplemental Figure 5F. Pathway analysis of the Retinoblastoma gene in cancer in CK-stimulated uNK versus CK-stimulated pNK.

Accepted Manuscript published as REP-18-0509.R1. Accepted for publication: 03-Jun-2019

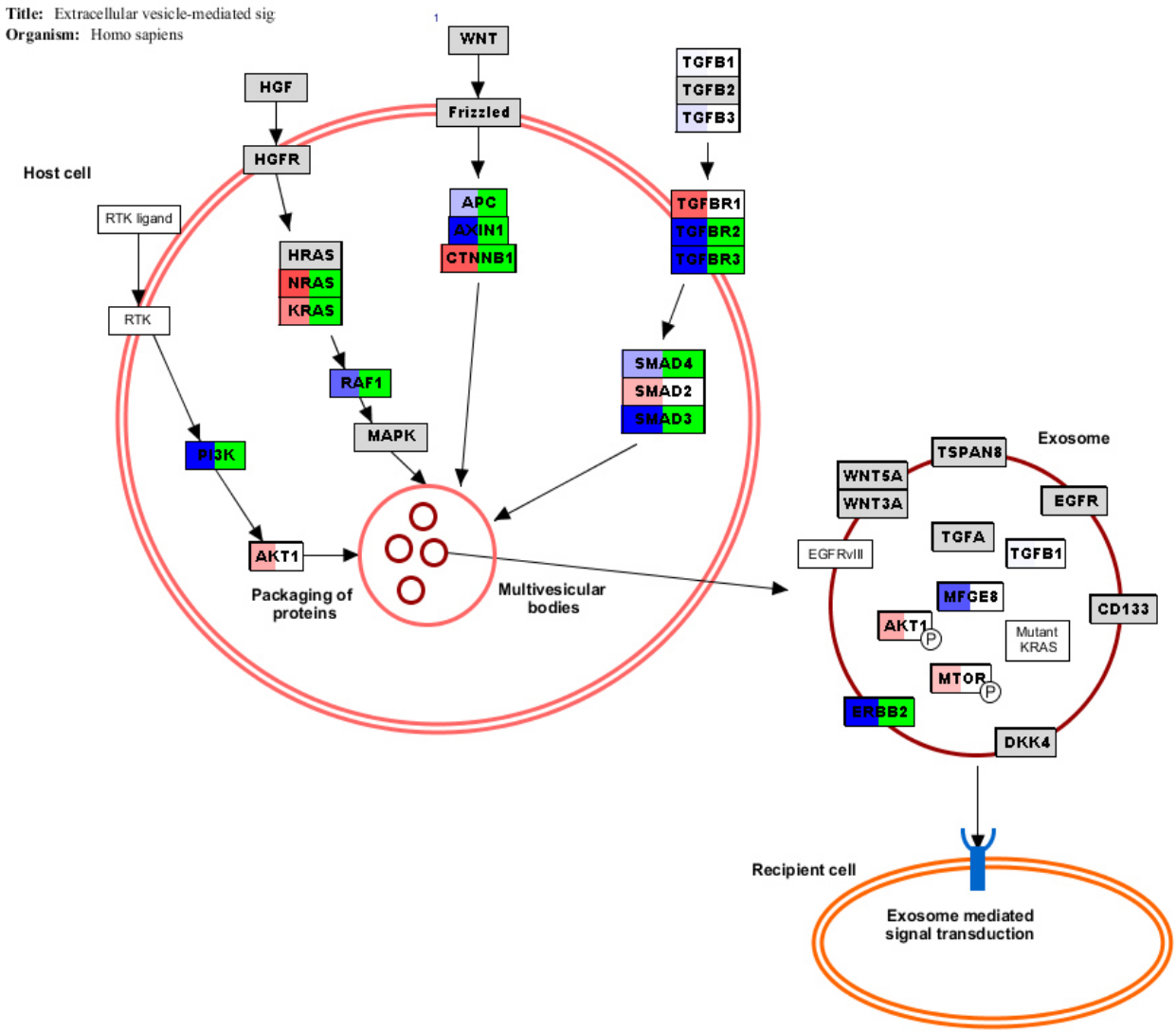

Supplemental Figure 5G. Pathway analysis of extracellular vesicle-mediated signaling in recipient cells in CK-stimulated uNK versus CK-stimulated pNK.

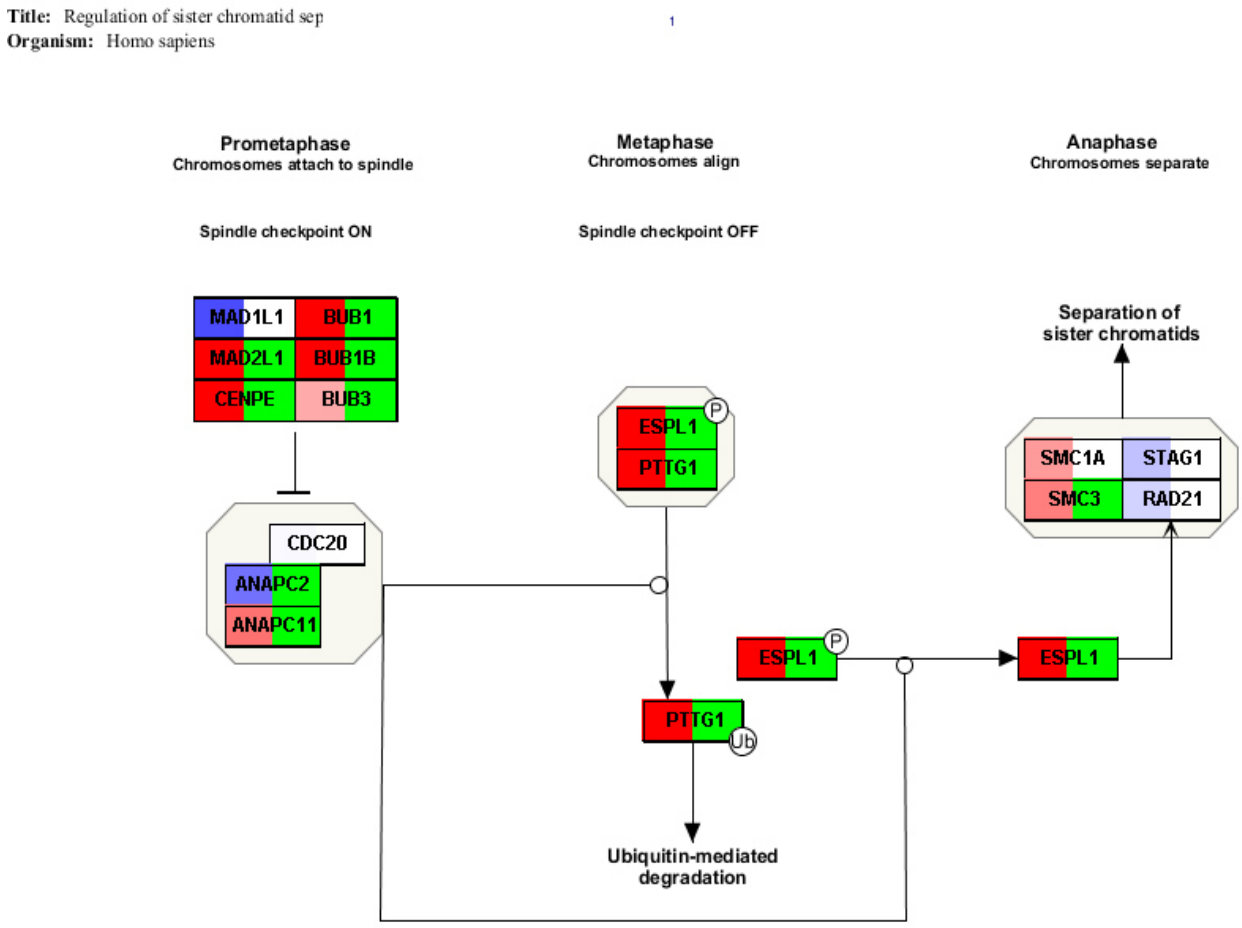

Supplemental Figure 5H. Pathway analysis of Regulation of sister chromatid separation at metaphase-anaphase transition in CK-stimulated uNK versus CK-stimulated pNK.

Accepted Manuscript published as REP-18-0509.R1. Accepted for publication: 03-Jun-2019

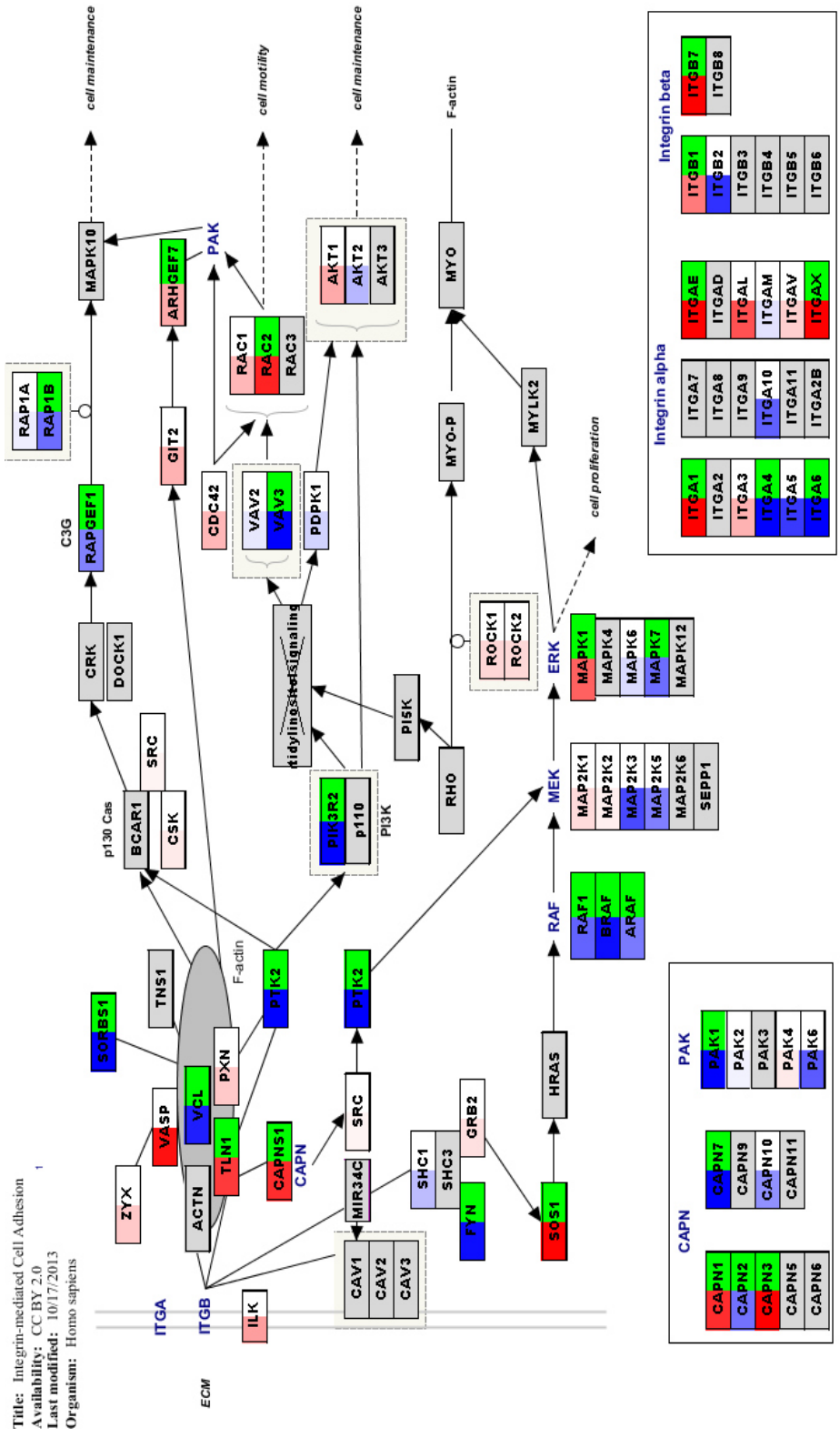

Supplemental Figure 5I. Pathway analysis of Fluoropyrimidine Activity in CK-stimulated uNK versus CK-stimulated pNK.

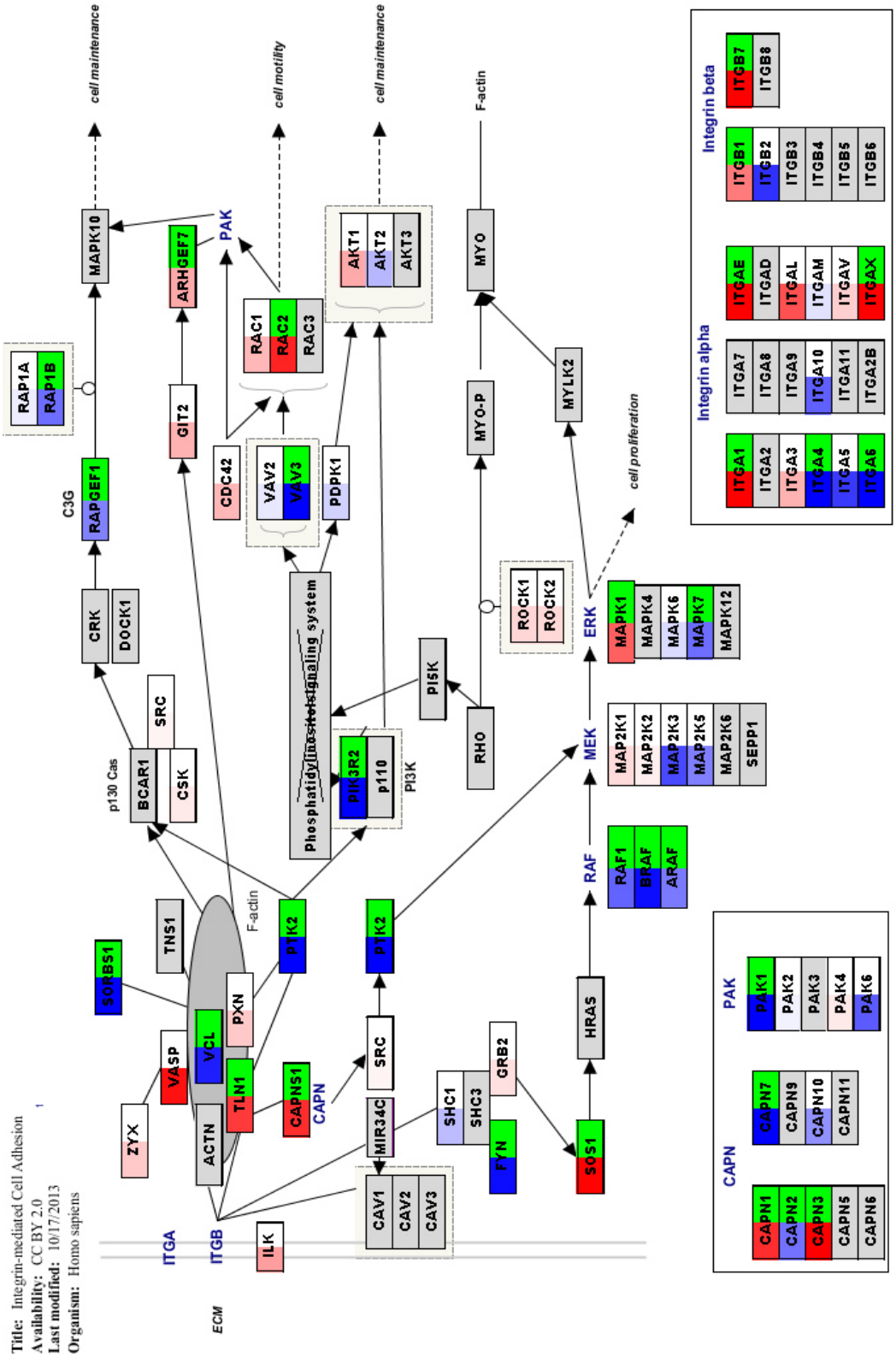

Supplemental Figure 5J. Pathway analysis of Integrin-mediated Cell Adhesion in CK-stimulated uNK versus CK-stimulated pNK.

Accepted Manuscript published as REP-18-0509.R1. Accepted for publication: 03-Jun-2019

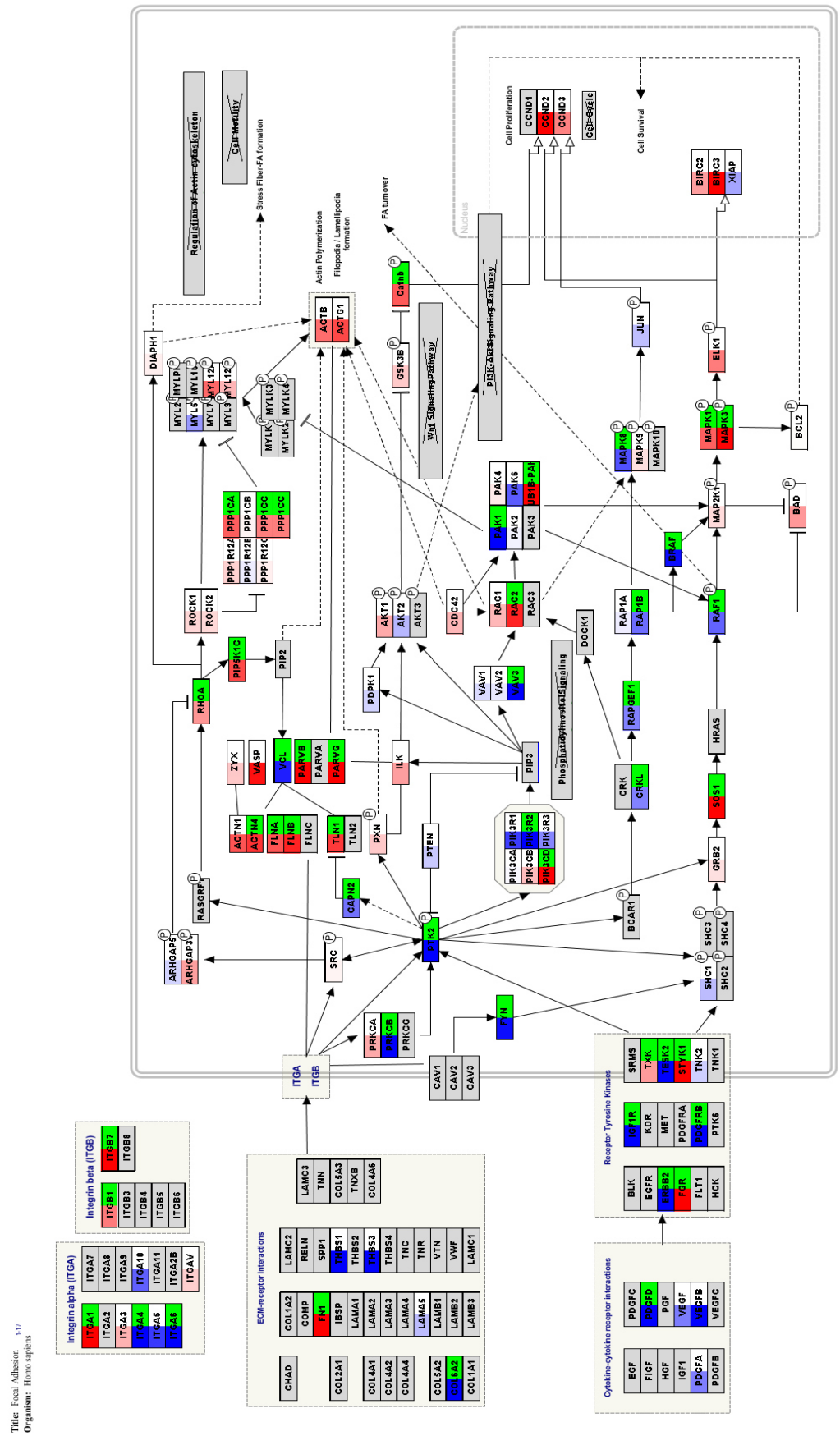

Supplemental Figure 5K. Pathway analysis of Focal Adhesion in CK-stimulated uNK versus CK-stimulated pNK.

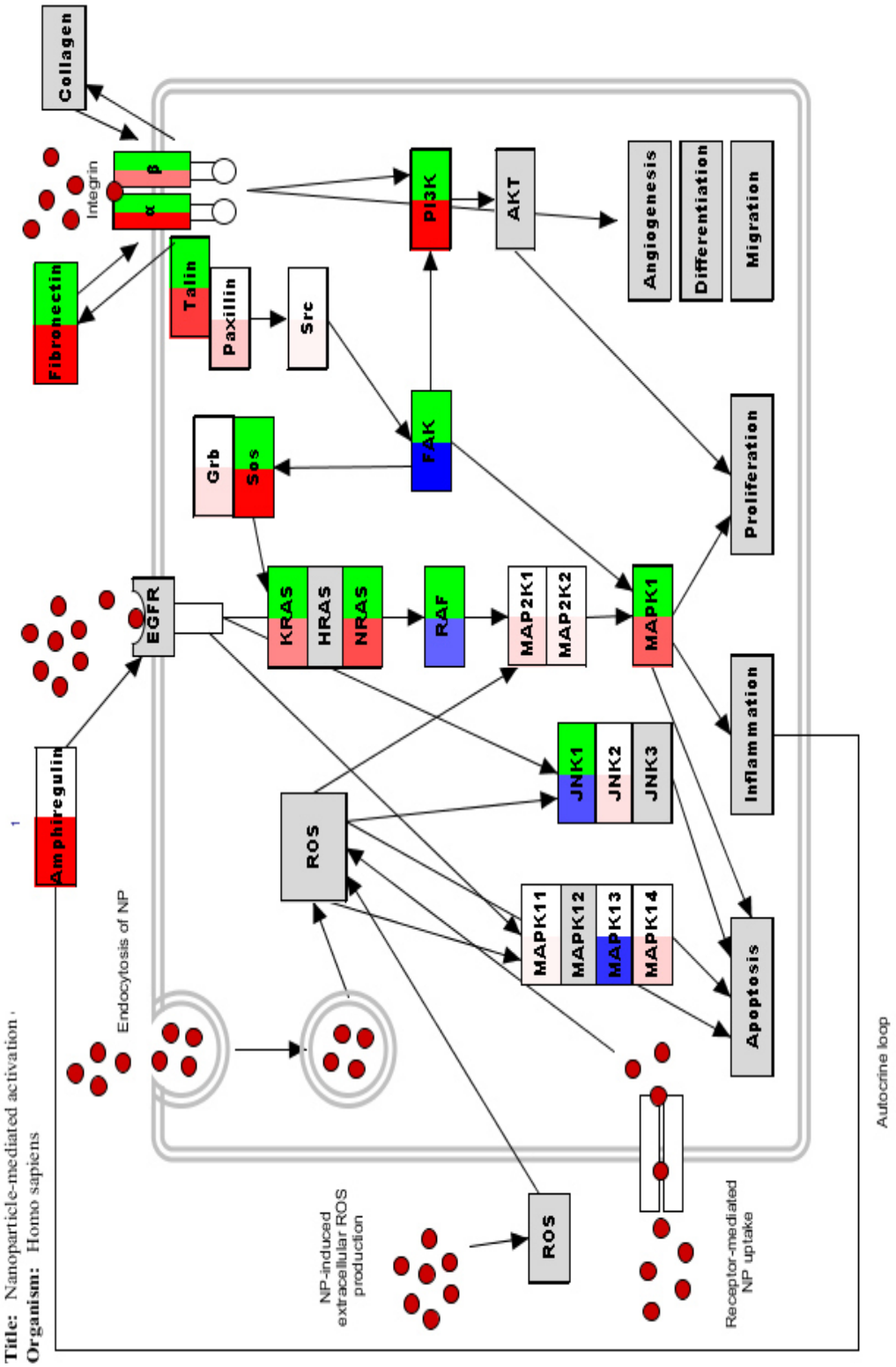

Supplemental Figure 5L. Pathway analysis of the Nanoparticle-mediated activation of receptor signalling in CK-stimulated uNK versus CK-stimulated pNK.

Accepted Manuscript published as REP-18-0509.R1. Accepted for publication: 03-Jun-2019

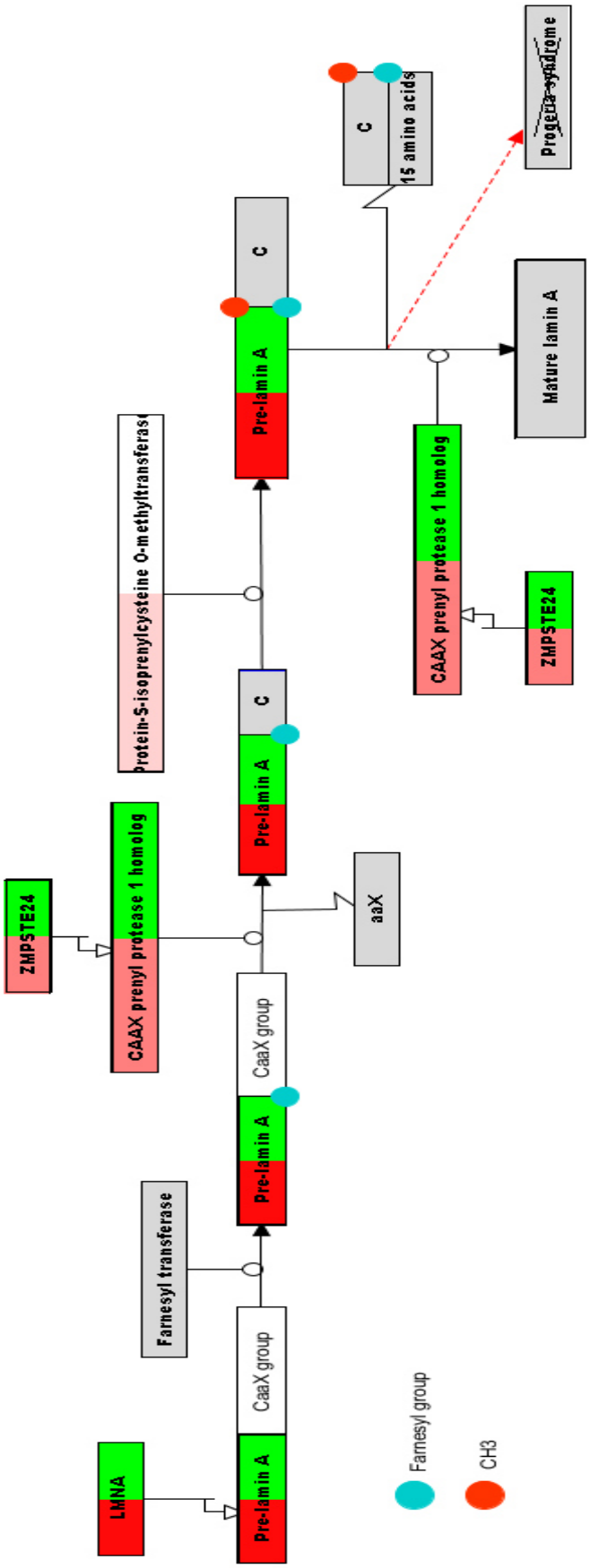

Supplemental Figure 5M. Pathway analysis of the Lamin A-processing pathway signalling in CK-stimulated uNK versus CK-stimulated pNK.

Supplemental Figure 5N. Pathway analysis of Signal Transduction of S1P Receptor signalling in CK-stimulated uNK versus CK-stimulated pNK.

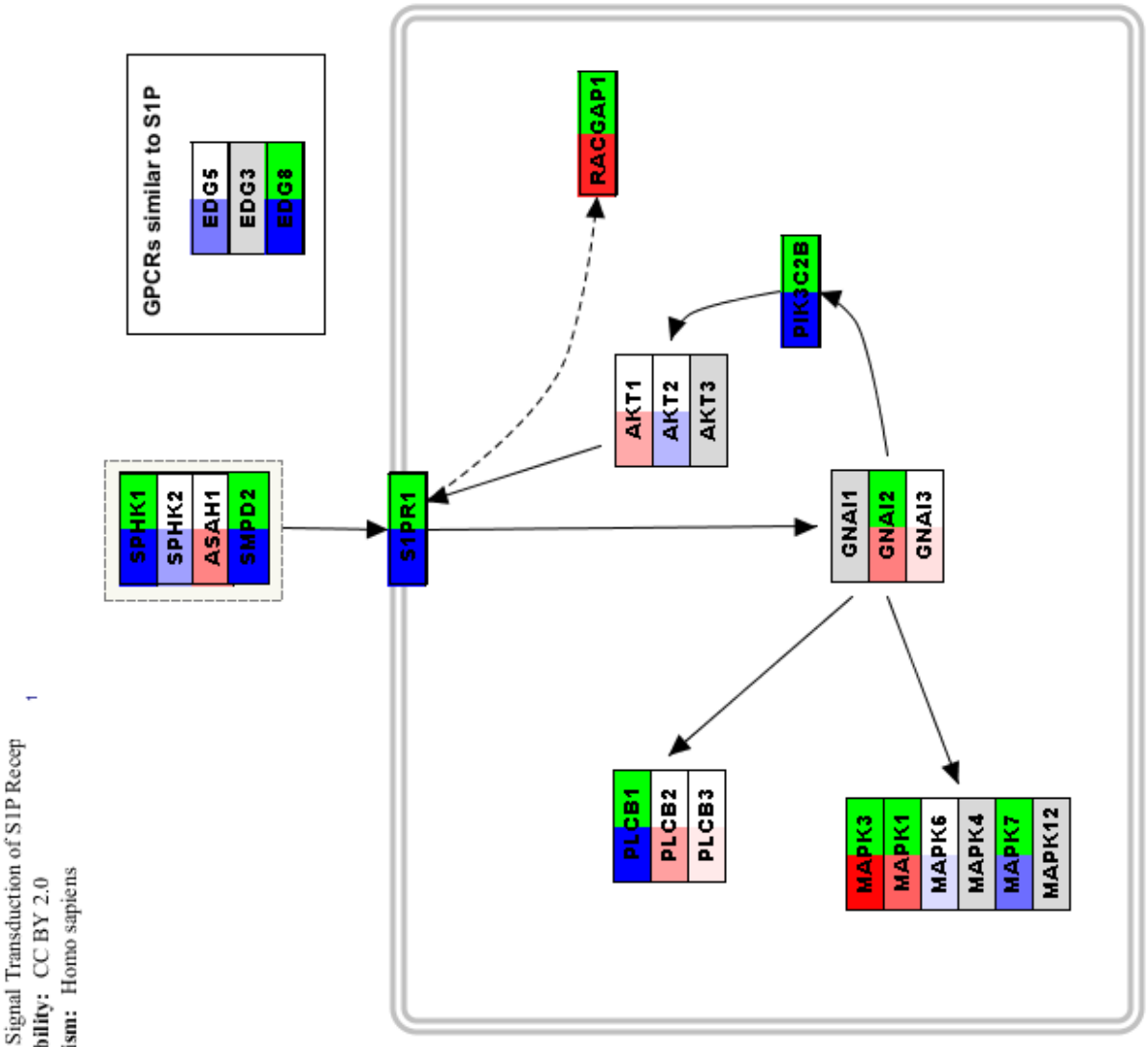

Accepted Manuscript published as REP-18-0509.R1. Accepted for publication: 03-Jun-2019

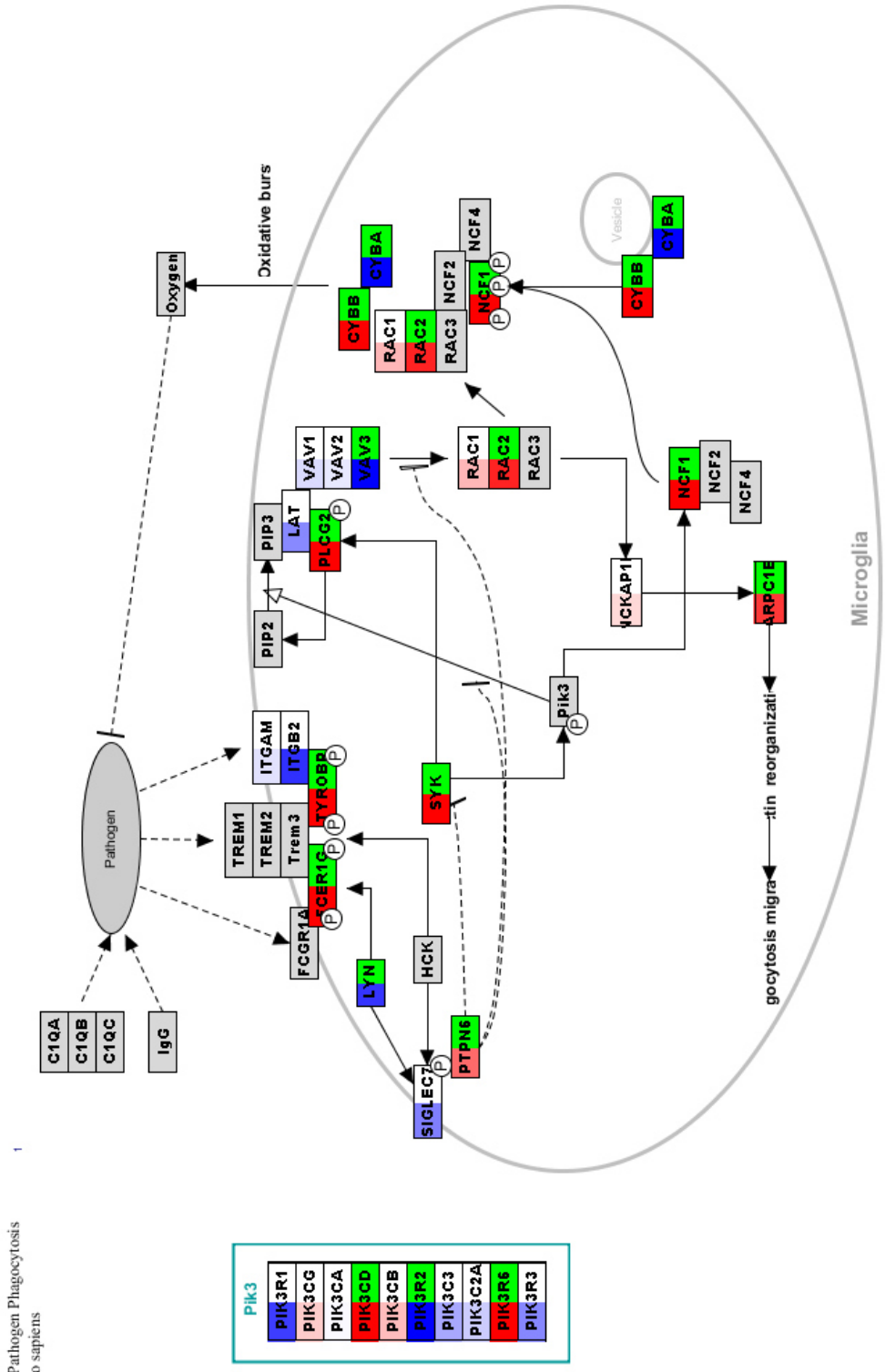

Supplemental Figure 5O. Pathway analysis of Microglia Pathogen Phagocytosis Pathway in CK-stimulated uNK versus CK-stimulated pNK.

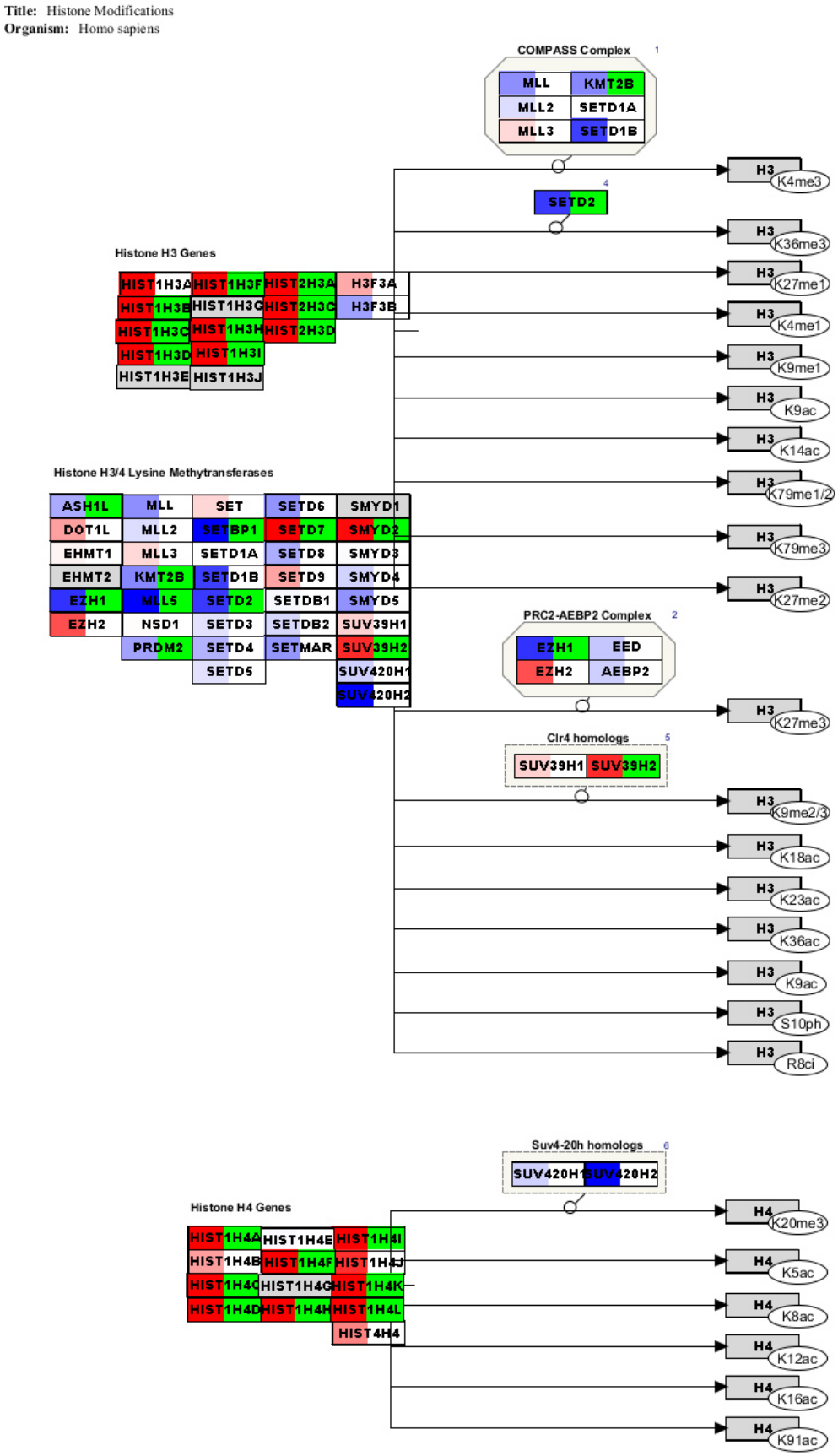

Supplemental Figure 5P. Pathway analysis of Histone Modifications in CK-stimulated uNK versus CK-stimulated pNK.

Accepted Manuscript published as REP-18-0509.R1. Accepted for publication: 03-Jun-2019

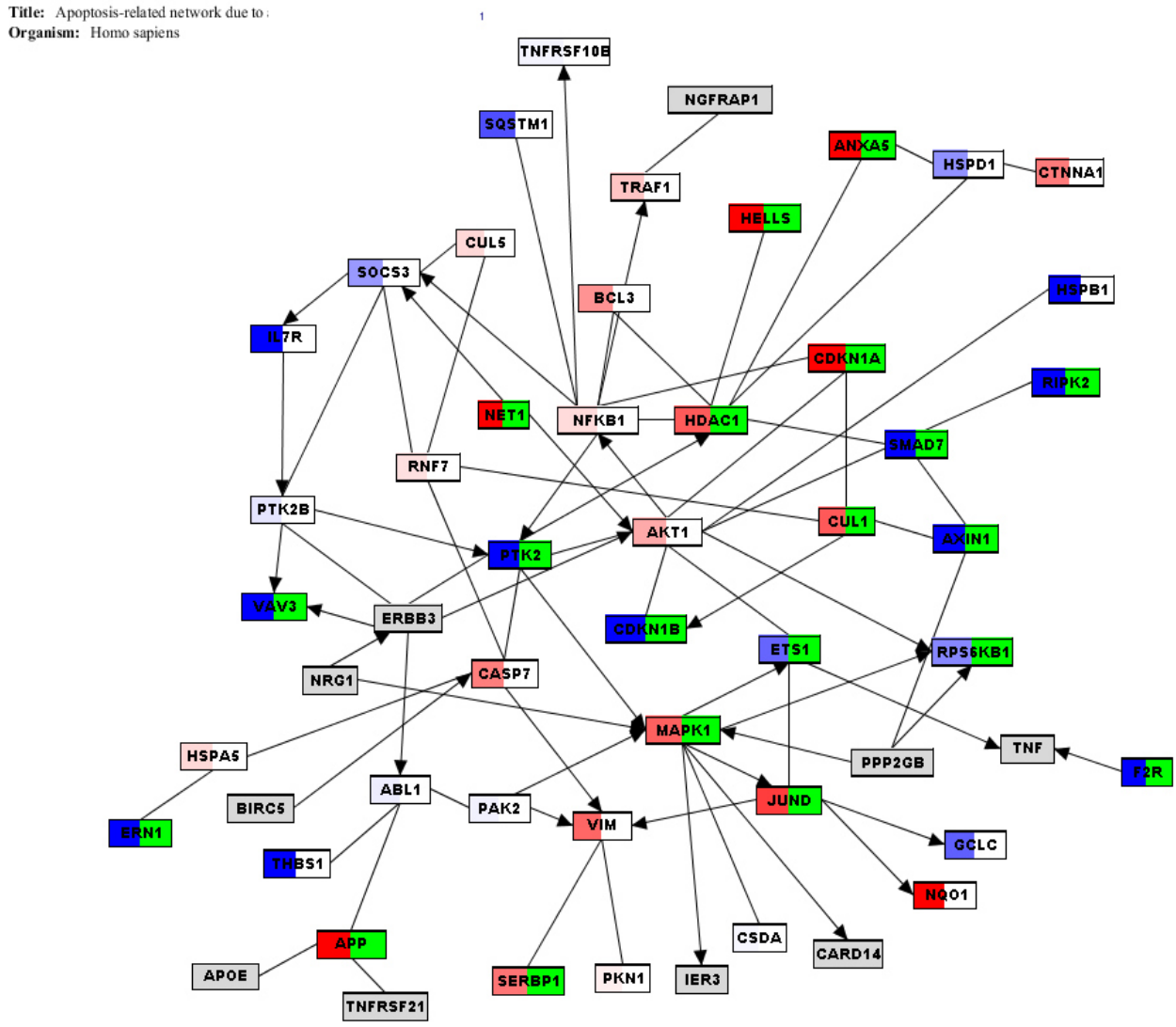

Supplemental Figure 5Q. Pathway analysis of Apoptosis-related network due to altered Notch3 in ovarian cancer in CK-stimulated uNK versus CK-stimulated pNK.

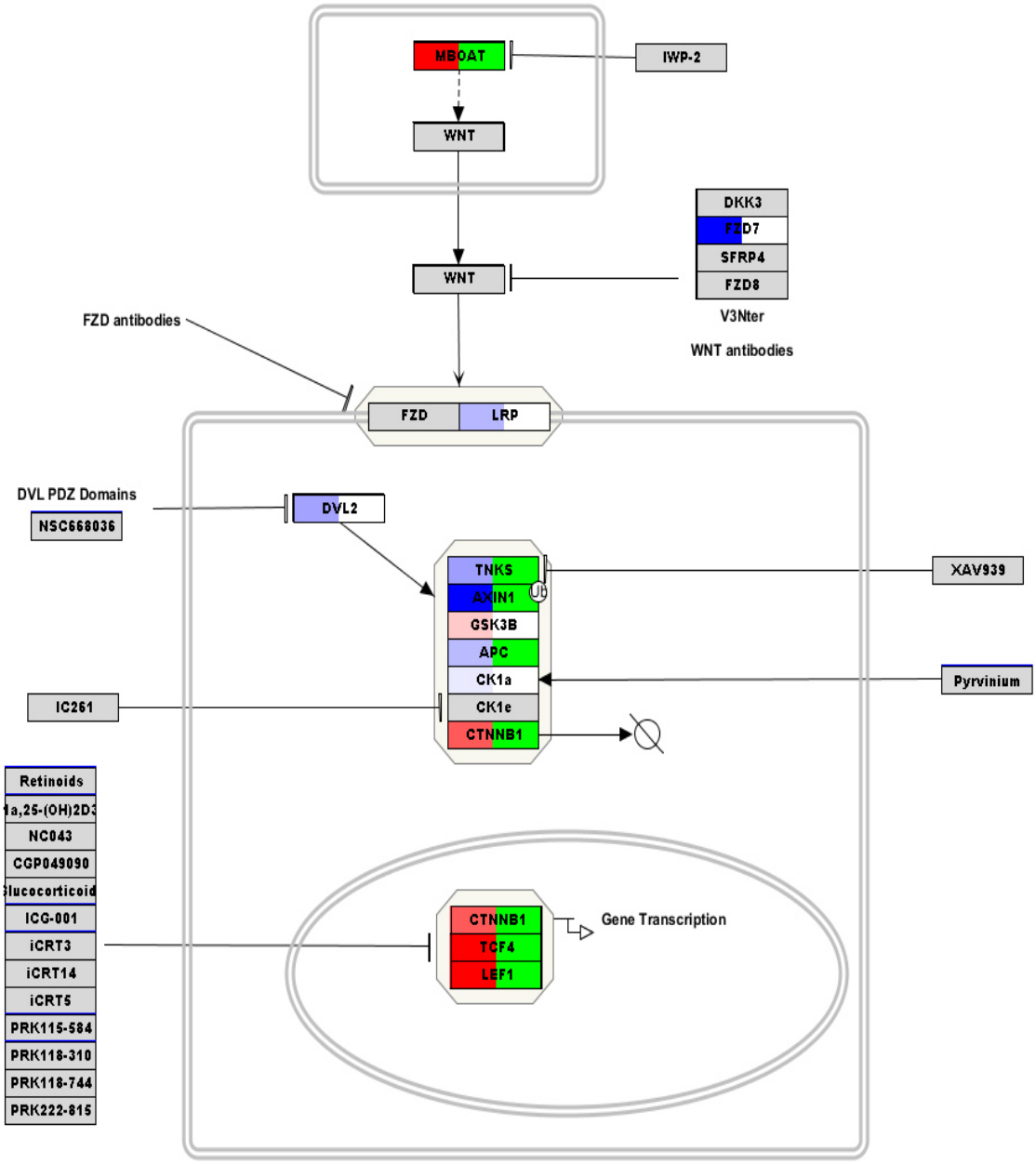

Supplemental Figure 5R. Pathway analysis of Regulation of Wnt/B-catenin Signaling by Small Molecule Compounds in CK-stimulated uNK versus CK-stimulated pNK.

Accepted Manuscript published as REP-18-0509.R1. Accepted for publication: 03-Jun-2019

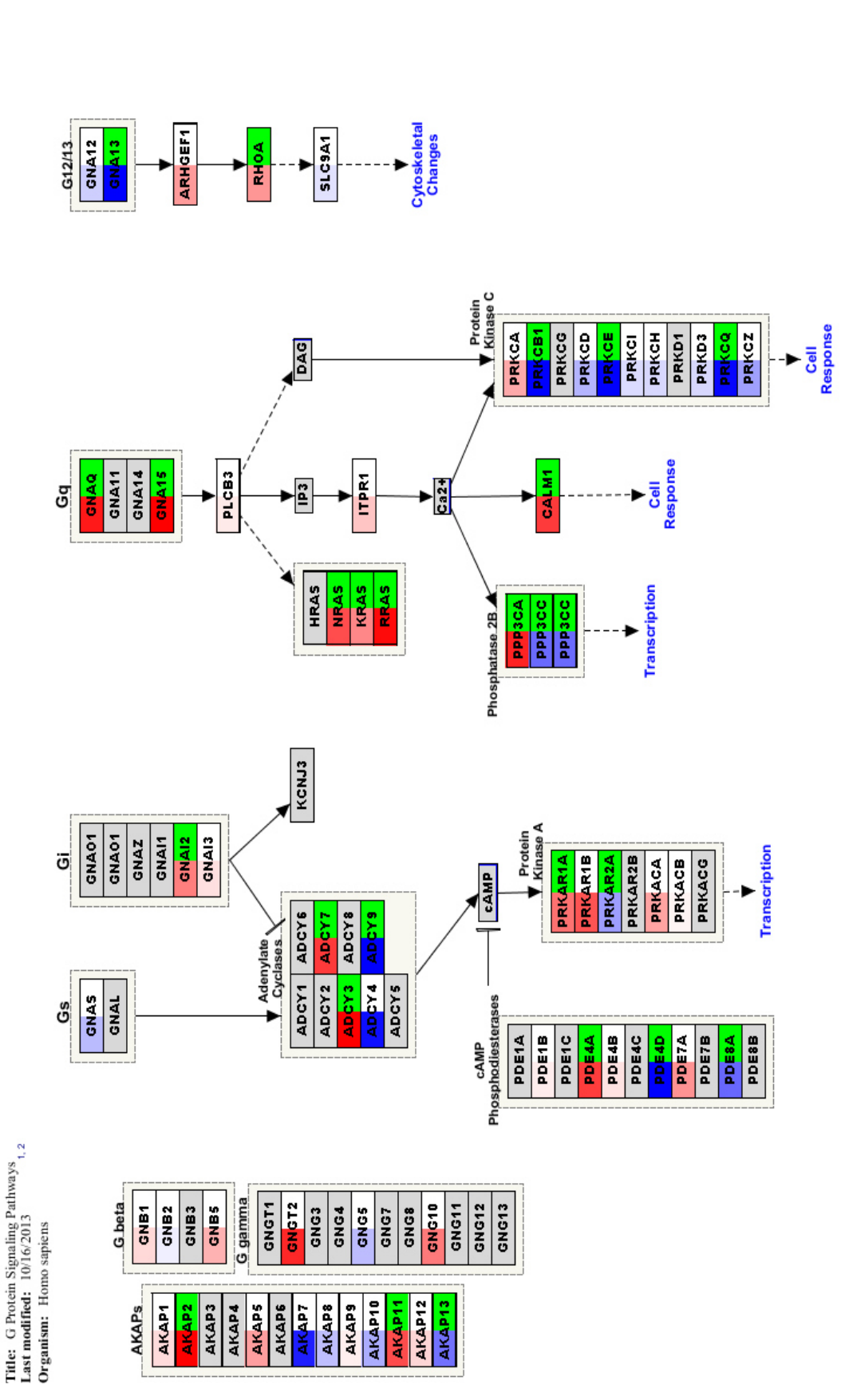

Supplemental Figure 5S. Pathway analysis of G Protein Signaling Pathways in CK-stimulated uNK versus CK-stimulated pNK.